Marble quarries in Delos Island (Greece): a geological characterization

Tommy Vettor, Violaine Sautter, Laurent Jolivet, Jean-Charles Moretti, Sylvain Pont

BSGF - Earth Sciences Bulletin 2022, 193, 16
© T. Vettor *et al.*, Published by EDP Sciences 2022
https://doi.org/10.1051/bsgf/2022014

BSGF
Earth Sciences Bulletin
Available online at:
www.bsgf.fr

Open Access

Marble quarries in Delos Island (Greece): a geological characterization

Tommy Vettor[1,*], Violaine Sautter[1], Laurent Jolivet[2], Jean-Charles Moretti[3] and Sylvain Pont[1]

[1] Institut de Minéralogie, de Physique des Matériaux et de Cosmochimie (IMPMC), UMR CNRS 7590, Muséum national d'Histoire naturelle, Sorbonne Université, 75005 Paris, France
[2] ISTeP, UMR CNRS 7193, Sorbonne Université, 75252 Paris, France
[3] CNRS, Institut de Recherche sur l'Architecture Antique, Université Lumière Lyon 2, MOM, 69365 Lyon, France

Received: 12 March 2022 / Accepted: 20 July 2022 / Publishing online: 11 September 2022

Abstract – Traces of extraction in Delian marble quarries attest their exploitation during Antiquity. A preliminary non-destructive provenance study confirmed the presence of indigenous marble in Delos constructions. In contrast, Delos marble quarries have not been geochemically described so far. Therefore, a detailed (1/5000 scale) geological mapping and cross-sections were performed in the four Delian marble quarries in order to better determine their dimension and to estimate the volume of extracted marble. The surface of the quarries was revised into up to six times larger areas, increasing the extracted volume estimations. Quarries were sampled and studied with mineralo-petrographic (optical and electronic microscopy, X-Ray Diffraction) and isotopic ($\delta^{13}C$ and $\delta^{18}O$) characterization. Three categories were observed, *i.e.*, a coarse whitish to bluish marble, a fine yellowish dolomitic marble and marble with giant white and blue calcite crystals. The Maximum Grain Size associated with oxygen and carbon isotopic ratios showed a good potential to distinguish Delian marbles from most of the main Mediterranean marbles used during Antiquity. However, geochemical elemental analyses such as trace elements analysis could supplement Delian marble characterization which will benefit future provenance studies.

Keywords: marble / quarries / Delos Island / Antiquity period / petrographic and isotopic characterization / archaeometry

Résumé – Les carrières de marbre de l'île de Délos (Grèce) : une caractérisation géologique. Des traces d'extraction dans les carrières de marbre de Délos attestent de leur exploitation durant l'Antiquité. Une première étude géochimique non destructive a permis d'identifier du marbre dans les constructions de Délos. Toutefois les carrières n'avaient jamais fait l'objet d'une étude géochimique détaillée jusque-là. Par conséquent, une carte géologique détaillée (échelle 1/5000) ainsi que des coupes géologiques ont été réalisées dans les quatre carrières de marbre afin de mieux cerner la dimension des carrières et les volumes de marbre qui en ont été extraits. La surface des carrières a été largement revue à la hausse, atteignant jusqu'à six fois la surface de la précédente cartographie des carrières, ce qui augmente donc considérablement le volume théorique de marbre extrait à Délos. Les carrières ont été échantillonnées et étudiées par une caractérisation minéralo-pétrographique (microscopie optique et électronique, diffraction de rayons X) et isotopique ($\delta^{13}C$ et $\delta^{18}O$). Trois catégories ont été observées, à savoir un marbre grossier blanchâtre à bleuté, un marbre dolomitique jaunâtre fin et un marbre à cristaux géants de calcite blanche et bleue. La taille maximale des grains associée aux rapports isotopiques de l'oxygène et du carbone ont montré un bon potentiel pour distinguer les marbres déliens de la plupart des principaux marbres Méditerranéens utilisés durant l'Antiquité. Cependant, des analyses géochimiques élémentaires comme l'analyse des éléments traces dans la calcite/dolomite pourraient apporter des éléments discriminants dans la caractérisation des marbres autochtones, ce qui profitera à de futures études de provenance des marbres.

Mots clés : marbre / carrières / Délos / Antiquité / caractérisation pétrographique et isotopique / archéométrie

*Correspondence: tommy.vettor@edu.mnhn.fr

1 Introduction

1.1 Context of the study

Marble was used extensively in architecture during antiquity in Archaic, Classic, Hellenistic and Roman periods. Ancient quarries are numerous around the Mediterranean basin in Italy, Greece and Turkey (Kokkorou-Aleura *et al.*, 2014). They provided a very large volume of marble on the antique trade routes. These exchanges explain a great diversity of marbles in ancient constructions around the Mediterranean basin, combining native marbles with imported marbles. White marbles are the most challenging in terms of provenance determination as they were used extensively in ancient artefacts (monument and sculpture) but have no characteristic macroscopic features except their grain size. To decide whether marbles are indigenous material or imported therefore requires multi-technic investigations.

Marble provenance tracing dates back to the 19th century as evidenced by the pioneer work of Lepsius (1890) which has since become a reference in marble provenance studies. Today studies dedicated to ancient marble traceability are numerous and rely essentially on a combination of a variety of analytical techniques such as petrographic examination of thin sections, X-ray diffraction and determination of trace element and C & O stable isotopic ratios on powder of the same sample (Lazzarini, 2004 and references therein). Such combination takes benefits of the most up to date existing data base for the main Mediterranean marbles from antique quarries active in Greek and Roman time (Zoeldfoeldi, 2011; Antonelli and Lazzarini, 2015; Attanasio *et al.*, 2015; Poretti *et al.*, 2017).

This study is dedicated to indigenous marbles in the architecture of Delos City hosting the Apollo sanctuary, located right in the middle of the Cyclades archipelago (Aegean Sea, Greece). Although a variety of imported marbles from Paros, Naxos, Tinos, Pentelicon has been identified, so far the use of local marbles remains an open question. According to visual inspections and some preliminary marble investigations, it seems that local marbles were also used in the architecture (Cayeux, 1911; Vallois, 1944; Fraisse and Kozelj, 1991; Vettor *et al.*, 2021). This paper presents the results of detailed mapping (scale 1/5000) of the marble outcrops identified in Delos where five ancient marble quarries have been recognized (Cayeux, 1911; Hadjidakis *et al.*, 2003). In addition, a reassessment of excavated marble has been made. Finally, detailed petrographic and isotopic surveys have been performed to complete the existing database on Greek marbles (Attanasio *et al.*, 2006, 2015; Antonelli and Lazzarini, 2015).

1.2 Geological settings

The Cyclades Archipelago forms a wide sub-marine plateau in the centre of the Aegean Sea where a series of islands such as Tinos, Delos, Mykonos, Rhenia, Paros and Naxos show the apex of Metamorphic Core Complexes (MCCs). They belong to the Attic-Cycladic metamorphic belt exhumed along low angle detachments (Lister *et al.*, 1984; Gautier and Brun, 1994; Rabillard *et al.*, 2018) during the Oligocene/Miocene extension episode. These metamorphic rocks have first recorded an Eocene (55–35 Ma) high-pressure and low-temperature metamorphism evidenced by blue schist-eclogite facies parageneses (Altherr *et al.*, 1979; Bonneau, 1982; Bröcker and Franz, 1994; Ring *et al.*, 2001; Parra *et al.*, 2002; Jolivet *et al.*, 2004a, 2004b; Jolivet and Brun, 2010) related to the convergence between African and Eurasian plates accommodated by subduction of the small Pindos oceanic basin. It is then overprinted by Oligocene/Miocene (30–8 Ma) medium pressure and temperature evidenced by greenschist and amphibolite facies parageneses. It locally reaches partial melting, recording the Aegean back-arc extension/exhumation controlled by a 700 km slab retreat of the Hellenic subduction (*e.g.*, Jolivet and Brun, 2010). Aegean granitoid plutons intrude the MCCs during a short period between 16 and 8 Ma (Jolivet *et al.*, 2015). In this context, marbles occur associated in sequence with gneiss and metabasite within the Cycladic Blueschist Unit surrounding the thermal domes locally intruded by granitic plutons.

Delos is one of the smallest Cycladic Islands (5 km long and 1.3 km wide). It belongs to the Mykonos–Delos–Rhenia MCC (Jolivet *et al.*, 2021) exhumed as a high-temperature gneissic dome during back arc extension (20 to 8 Ma). This stage ends up with the syn-kinematic piercing of the dome by a granitic-granodioritic type I laccolith 11.1–9.5 Ma ago outcropping essentially in Delos, Mykonos and SE Rhenia, which substratum is otherwise dominated by gneissic material (Altherr and Siebel, 2002 and reference therein, Denèle *et al.*, 2011; Jolivet *et al.*, 2021, Fig. 1). This laccolith intruding the Cycladic Blueschists Unit (CBU) results from successive pulses of magma in a very short time interval (Lucas, 1999) during the post-orogenic back-arc extension stage. In Delos, the granitic material forms more than 4/5 of the island substratum, the intruded gneissic material being restricted to the north and to large inclusions within the pluton. The gneiss is more or less migmatitic and may originally represent the Cycladic basement of Hercynian age (327 ± 4 Ma to 295 ± 44 Ma: Keay, 1998). Within the Delos granitic pluton, diversified highly deformed metamorphic country rocks from the Cycladic Blueschist Unit cover appear as small metric to decametric enclaves forming approximately 5% of the island (Cayeux, 1911). They consist of interbedded foliated layers of marble, amphibolite, and gneiss, initially (55–35 Ma) buried under blueschist facies conditions then (30–15 Ma) retrograded during exhumation under amphibolite/greenschist conditions. At least five ancient marble quarries (Fig. 1), about a hundred meters long, have been identified throughout Delos Island (Fraisse and Kozelj, 1991; Chatzidakis *et al.*, 1997; Hadjidakis *et al.*, 2003; Kokkorou-Aleura *et al.*, 2014) among the 39 ancient quarries recently indexed. Preliminary volume estimations determined from topography study of the quarries give a first order estimation of 174 000 m^3 of extracted material.

1.3 Delos in ancient times

Delos, the mythological birthplace of Apollo and Artemis, is well known for its exceptionally well-preserved archaeological site. Given its central position, it has been inhabited since the second half of the 3rd millennium. Excavation by the French School of Athens (École française d'Athènes, EFA) started in 1873. Ruins of more than three millennia of human

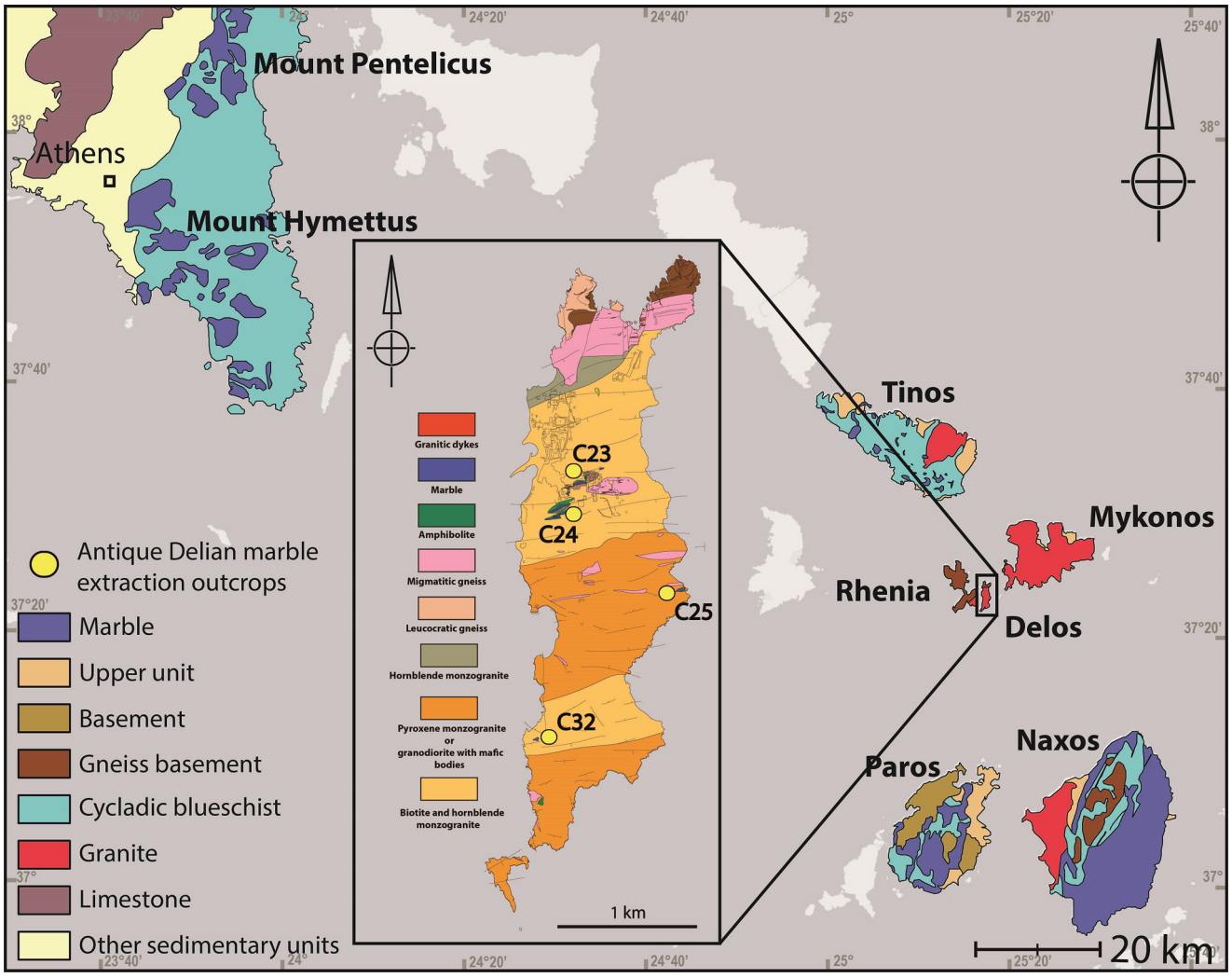

Fig. 1. Geological map of Delos modified from Jolivet *et al.* (2021) in its simplified regional context. The yellow circles locate marbles quarries C23, C24, C25 and C32.

occupation, with an acme at the end of the first century BC, are visible in the northwestern part of the island. The antique city has expanded over 80 hectares but only 30 of them have been excavated so far (Fig. 1). This small island became a famous religious sanctuary during the seventh century BC and then (167 BC) a major free harbour, evolving into a key trading point during Antiquity (Bruneau and Ducat, 2005). Merchandises from the Cyclades, Attique, and even further (Italy, Asia Minor, Egypt, etc.) were circulating through Delos harbour.

Religious, commercial, and residential buildings appear to be essentially built from granite, gneiss, and marble. Preliminary estimations indicate that a minimum volume of 500 000 m^3 was necessary to account for the marble excavated so far. However, as mentioned above, indigenous marble extracted from local quarries does not exceed 174 000 m^3, which is three to five times less than the required volume excavated so far for the ancient buildings. As Delos was a key trading point, possibilities for marble import are numerous. Building site accounts, generally carved on marble slabs, specify exchanges with Aegean Islands such as Paros, as well as the continental Athenian region (Fig. 1). The purpose of the present study is to re-evaluate the ratio of local marbles *versus* the imported ones by detailed mapping at 1/5000 of the five quarries initially described by Cayeux (1911), described later on and labelled Qm1 to Qm5 by Hadjidakis *et al.* (2003).

2 Material and methods

2.1 Material

Sixty-one samples from the Delian marble quarries were investigated in this study.

The number of samples depends on the dimension and the geological complexity of a given quarry. The quarry nomenclature initially defined by Hadjidakis *et al.* (2003) was revised into a new terminology incorporating all 39 quarries recently indexed in Delos. The theatre and Inopos reservoir marble quarries Qm4 and Qm5 were merged and

renamed C23 as they belong to the same geological outcrop. The other marble quarries were renamed: Qm3 = C24; Qm2 = C25; Qm1 = C32. Thin sections and powders obtained with an agate mechanical grinder were produced from the four marble quarries in order to perform a petrographic and geochemical characterization.

2.2 Methods

2.2.1 Mapping

The first detailed geological study of Delos dates from 1911 (Cayeux, 1911) and provided a preliminary 10 000th scale geological map of Delos. Five marbles outcrops were identified within the granitic laccolith and geological sections were proposed. Since then, more recent studies focused on the granitoid laccolith emplacement and its detailed petrography (Lucas, 1999). A new 10 000th scale geological map was produced (Pe-Piper *et al.*, 2002) while Jolivet *et al.* (2021) have revised this map focusing on the geometry and the deformation within the migmatitic core of the Mykonos–Delos–Rhenia MCC and interaction with the main granitoid laccolith outcropping in Delos. A north-south cross-section through Delos (Fig. 9 in Jolivet *et al.*, 2021) shows parallel steep E-W foliation in granitoids and metamorphic enclaves.

In this study, we performed detailed 5000th scale geological mapping of marble lenses and cross-sections in each marble quarry. Marble lens thicknesses mentioned in this article refer to the "true" thickness T of marble lenses measured perpendicular to foliation. These have been calculated from the dip α of the lenses and their outcropping/apparent thickness T_a following the equation:

$$T = \sin(\alpha).T_a.$$

2.2.2 Petrographic analyses

Mineralo-petrographic analyses are of fundamental importance to characterise marbles and determine their genesis, *e.g.*, type of metamorphism (burial, contact) and grade (low, medium, high).

2.2.2.1 Maximum grain size (MGS)

One of the most commonly used parameters in marble provenance studies is the Maximum Grain Size (MGS) of the rock-forming calcite and dolomite crystals. Such a parameter is linked to the achieved grade of metamorphism. Attanasio *et al.* (2006) published the most comprehensive database of MGS with more than 1300 samples. For a long time, it remained a visually estimated parameter. We have directly measured the MGS of calcite/dolomite grains in the field with a portable microscope DINO-LITE model AM7515MZT. This model is equipped with a linear polarizer and an IR cut filter over 650 nm with a x20 to x220 magnification capacity. Statistically speaking, MGS measurements used in this article are based on six pictures per marble.

2.2.2.2 Optical and electron microscopy

Thin sections were analysed under a polarising microscope in order to determine the rock fabric, the shape of boundaries between calcite and dolomite, the grain size, shape and distribution, as well as accessory minerals (such as quartz or micas).

Thin sections were also analysed with a scanning electron microscope (TESCAN VEGA II LSU) coupled with an energy dispersive X-ray spectrometer (SEM-EDS) at the *Plateforme de Microscopie Électronique (PtME) du Muséum national d'Histoire naturelle*, Paris, France. EDS analyses were performed under high vacuum conditions (5.10^{-3} Pa) at 15 keV on carbon-coated sections. The aim was to obtain information on the elemental composition of accessory phases not identified with polarising microscopy, accessory minerals being potentially discriminatory criteria (Capedri *et al.*, 2004; Capedri and Venturelli, 2004).

The distribution of average grain dimensions allows to distinguish two fabrics. A homogeneous fabric (homeoblastic HO) with roughly isometric grains and another one where the grain size varies greatly (heteroblastic HE). These fabrics are related to the type of metamorphism (equilibrium, non-equilibrium, polymetamorphism). Microscopic examinations primarily regard structure of isotropic or oriented rocks which may be classified as a function of their microstructure (mortar or mosaic). Another important information is the shape and contour of grains. The crystal boundary geometry is defined as polygonal, interlobate and amoeboid. As described by Moore (1970), polygonal corresponds to geometric straight contacts, interlobate corresponds to slightly curved contacts and amoeboid corresponds to sutured contacts, the grains being interlocked with each other. Such boundaries are evidence of an increasing degree of deformation and decreasing degree of recrystallization (Passchier and Trouw, 2005). Finally, it is important to qualify any internal crystal deformations such as undulose extinction and deformation of polysynthetic twins which are distinctive of dynamic recrystallization processes typically localized in shear zones or fractures.

2.2.2.3 X-ray diffraction (XRD)

Forty-nine powders were analysed by X-ray Diffraction with a BRUKER D2 PHASER diffractometer equipped with a Cu anode at the *Plateforme de Diffraction des Rayons X de l'IMPMC*, Paris, France, in order to determine global calcite/dolomite ratios and major and accessory minerals proportions. Data were acquired in the range 3°–100° 2θ with a step-size of 0.013° 2θ and a counting time of 1 s/step.

2.2.3 Isotope geochemical analyses

Analyses of stable isotopes of oxygen and carbon can help to determine the provenance of marble deposits (Attanasio *et al.*, 2006; Gärtner *et al.*, 2011 and references therein). They have therefore been extensively used for marble traceability. Moreover, one of the most important advantages of the method is that only small powder samples are needed for analyses (about 50 µg) which are suitable for archaeological purposes.

Isotope analyses were carried out at the *Service de Spectrométrie de Masse Isotopique du Muséum national d'Histoire naturelle*, in Paris, France (SSMIM). 45 µg of powder was subjected to four drops of pure phosphoric acid at 70 °C. The released carbon dioxide was analysed on a Thermo Kiel IV carbonate device interfaced with a Thermo Delta V

Advantage Isotope Ratio Mass Spectrometer (IRMS). The spectrometer used is equipped with a double collector allowing the simultaneous measurement of $^{13}C/^{12}C$ and $^{18}O/^{16}O$ isotope ratios. These ratios are expressed as $\delta^{13}C$ and $\delta^{18}O$ respectively according to the following equation:

$$\delta = \left[\frac{R_{sample}}{R_{s\ tandard}} - 1\right] * 1000.$$

R_{sample} and $R_{standard}$ corresponding to the isotopic ratios ($^{13}C/^{12}C$ and $^{18}O/^{16}O$) of the sample and the reference standard respectively. The standard chosen for carbon and oxygen is the Vienna-Pee Dee Belemnite standard. Data were corrected with the laboratory marble standard LM (Lycée Marceau with $\delta^{13}C = +2.130‰$ and $\delta^{18}O = -1.830‰$), normalized in keeping with the NBS19 international standard. Two standards are analysed every 10 measurements in order to detect any drift.

3 Geology and quarries

3.1 Geological mapping of marble lenses

The two largest marble quarries C23 (the theatre hill and the Inopos reservoir) and C24 (Ghlastropi hill) are located within the Hellenistic borders of the city, while the other two C25 and C32 are outside the site further south, respectively on the eastern and western coast. The quarries are located in ellipsoidal lenses which are of relatively small dimension, from 10 to approximatively 200 m. Their long axis is parallel to the main NE-SW stretching direction in the island. The marbles are foliated (Jolivet *et al.*, 2021) with foliation in the northern C23 and C24 dipping 10° to 70° to the south (~ 160 SE) while foliation in the southern ones are dipping to the north (~ 340 NW, 35° for C25, 80° to 90° for C32). Marbles are often associated with amphibolite and brown biotite-rich gneiss (Cayeux, 1911).

3.1.1 The Central quarry

Quarry C23 has been excavated from a single NE-SW trending 220 m long marble lens dipping about 30 degrees to the south (Fig. 2), with two main extraction areas (theatre hill and Inopos reservoir). The marble of this quarry is whitish to bluish and coarse grained. It is associated with a fine whitish to orange dolomitic marble (Fig. 3c). The marble is associated with brown gneiss and amphibolite layers, with folds overturned to the south (Fig. 2c) with their axes parallel to the granite lineation (Jolivet *et al.*, 2021). The contact between marble and amphibolite is a thin centimetre thick layer of pyroxenite, all along the lens. The folding leads to a strong variation in layer thickness. Thus the 5 m thick amphibolite layer thins to the south of the marble lens and disappears in its central part (Fig. 2b). Brown gneiss separating amphibolite from granite varies from 5 m thick to a few centimetres. In the centre of the theatre hill, marble reaches a maximum thickness of 12 m, where 7 m of coarse marble layer is associated with 5 m of dolomitic marble. Those two layers decrease to a 1 m thickness, at the western end of the theatre hill. The lens is crossed by a NW-SE fault at the Inopos reservoir (Fig. 2b). On the eastern side of the fault, marble is associated with a dark green amphibolite layer interstratified with light green pyroxenite and is perpendicularly cut by cm thick epidote veins (Fig. 3a). Amphibolite was excavated and directly used into local constructions (Fig. 3b). The Inopos part of the lens is intensely folded and the eastern section of the reservoir shows a strong boudinage between marble and mafic layers (Fig. 4a) as well as a fold leading to a dip inversion (Fig. 4b). A small 1 m thick enclave of yellowish dolomitic marble outcrops in brown gneiss, between the reservoir of Inopos and the temple of Isis (Fig. 2b). Two small marble lenses (20–40 m long) are visible to the west and east of the main lens. One of these outcrops in the middle of the theatre stands, with a dip of 75° to the south, lies in the core of a synform overturned to the south. The advanced weathering of a large part of the outcrop surface led to a low exploitation of this marble. The second lens is located to the north-east of the temple of Isis, where marble is in direct contact with the granite. This contact is marked by a quartz vein about thirty centimetres thick. This marble appears to have been quarried, with clearly visible traces of extraction. However, it is difficult to estimate its initial volume before extraction as the marble lies directly on granite.

3.1.2 The Ghlastropi hill quarry

Quarry C24 comprises two NE-SW trending marble lenses with their long axis parallel to granite lineation (Jolivet *et al.*, 2021), dipping about 30 degrees to the south, crossed by two NW-SE faults identifiable by fault breaches in the marble (Figs. 5b and 5c). The northernmost lens is about 165 m long and about 15 m thick, including a 4 m thick layer of dolomitic marble. The lens is in the core of a large folded enclave of NE-SW trending brown gneiss and amphibolite. The lens is actually a synform overturned to the south with a layer dip ranging from 25° to 50°. The thick layer of amphibolite (approximately 20 m) to the north of the lens decreases to 5 m to the south (Fig. 5c). Brown gneiss marks the contact between marble and amphibolite over a ten centimetre thick layer to the north of the lens, compared to about 5 m at its southern limit (Figs. 5b and 5c). The calcitic part of the marble lens is a white to bluish pluri-milimetric marble as in C23 (Fig. 3f). Dolomitic marble is very fine grained (infra-milimetric grain size) with a yellowish to orange colour, identical to the one outcropping in C23 (Fig. 4c). The southern 180 m long marble lens has undergone the highest degree of exploitation in the quarry. The 11 m thick layer of coarse white to blue marble also forms a synform enclave overturned to the south with a dip between 40° and 90°, with amphibolite layer whose thickness of 10 m to the north decreases towards the south to a few centimetres (Fig. 5c). This layer disappears in places at the southern contact of the lens, thus bringing the marble and granite into contact. This contact gives way to a skarn about ten centimetres thick containing large garnets. Only a thin decimetric layer of yellowish marble is still visible between calcitic marble and granite. The western part of the lens is deformed in a very tight, vertically hinged fold combined with granitic intrusions at the northern border of the lens. Thin layers of marble and pyroxenite are interbedded in the core of the fold showing a strong boudinage (Fig. 4d). Close to the southern contact with the granite the rim of the lens differs texturally from the rest of C24 by calcite grains up to 3 cm in diameter.

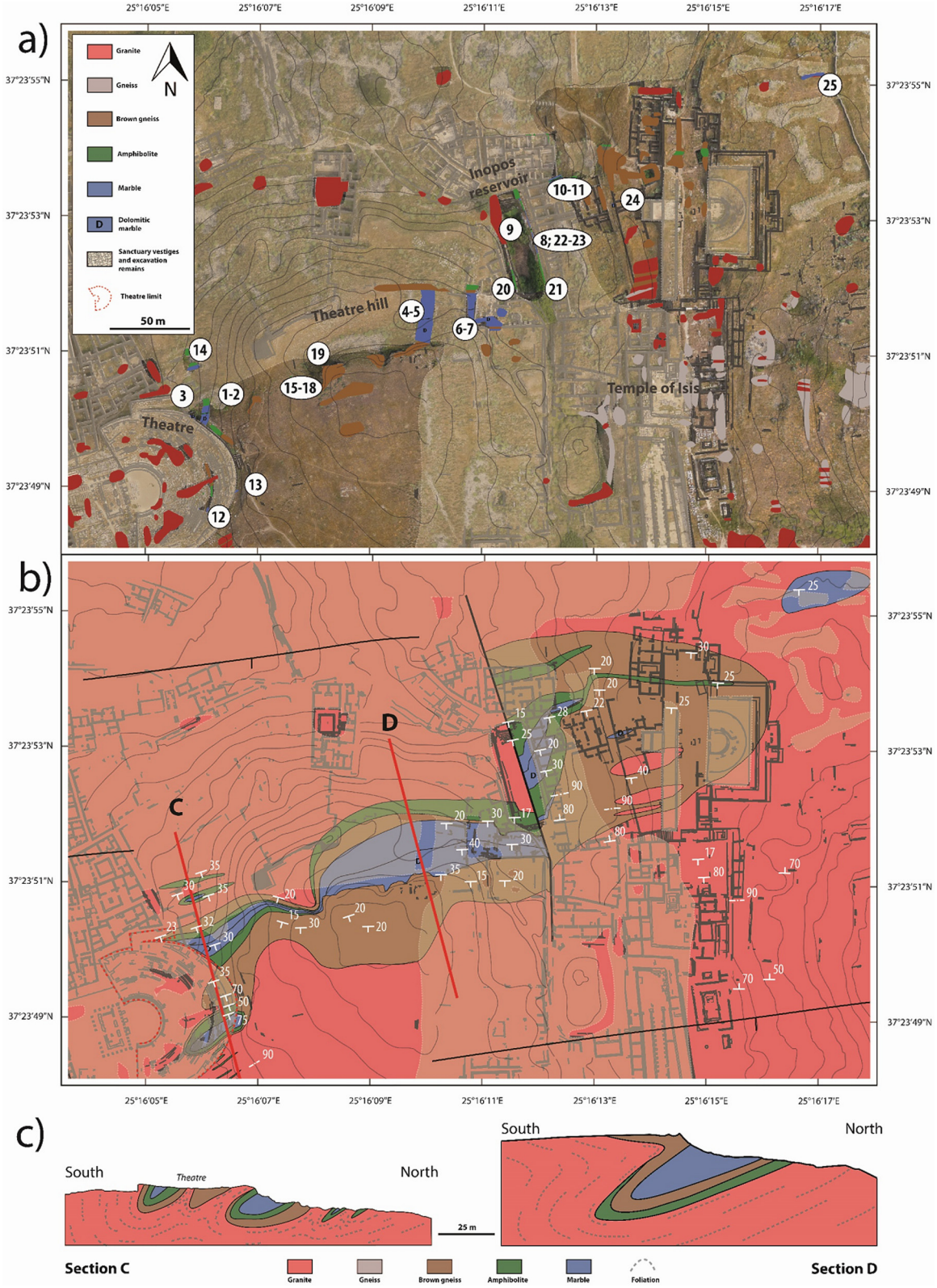

Fig. 2. (a) Location of the lithological outcrops and marble samples (n° 1 to n° 25) on the satellite map of the central quarry C23. The beige colour shows the areas covered by ruins or excavation debris, making the outcrops inaccessible; (b) 5000th scale geological map of the quarry C23. Delian constructions induce rapid variations in topography (as in the theatre), resulting in anomalous contacts on the map. The red lines locate the two cross sections C and D described below; (c) Cross sections C (left) and D (right) located in quarry C23.

Fig. 3. (a) Amphibolite outcrop in contact with white marble, inside the Inopos reservoir (C23); (b) Amphibolite stairs near the Inopos reservoir; (c) Yellowish dolomitic marble outcrop in the Inopos district (C23); (d) Extracted block of yellowish dolomitic marble, macroscopically very similar to the dolomitic marble of C24 and C23; (e) Yellowish dolomitic marble blocks in an Inopos district wall; (f) Bluish marble outcrop in Ghlastropi hill (C24); (g,h) Bluish marble very similar to the one outcropping in C23 and C24, respectively in a Ghlastropi hill wall (g) and inside the theatre (h).

3.1.3 The southernmost and easternmost quarries

A third quarry can be found on the east coast of the island, southwest of Mount Cynthus (C25, Figs. 6a–6c). Numerous traces of extraction are visible in the quarry in which three extraction sectors have been defined (Fraisse and Kozelj, 1991). The marble lens is 100 m long and 17 m thick at its maximum, in a synform with a NE-SW hinge parallel to the granite lineation with a dip of 35 degrees towards the north-west in contrast to the previous synforms. Marble from C25 is particularly recognisable with its large white to bluish centimetric crystals in a coarse matrix. Marble and granite are separated by a 5 m thick layer of fine grained amphibolite to the south of the lens and 1 m to the north.

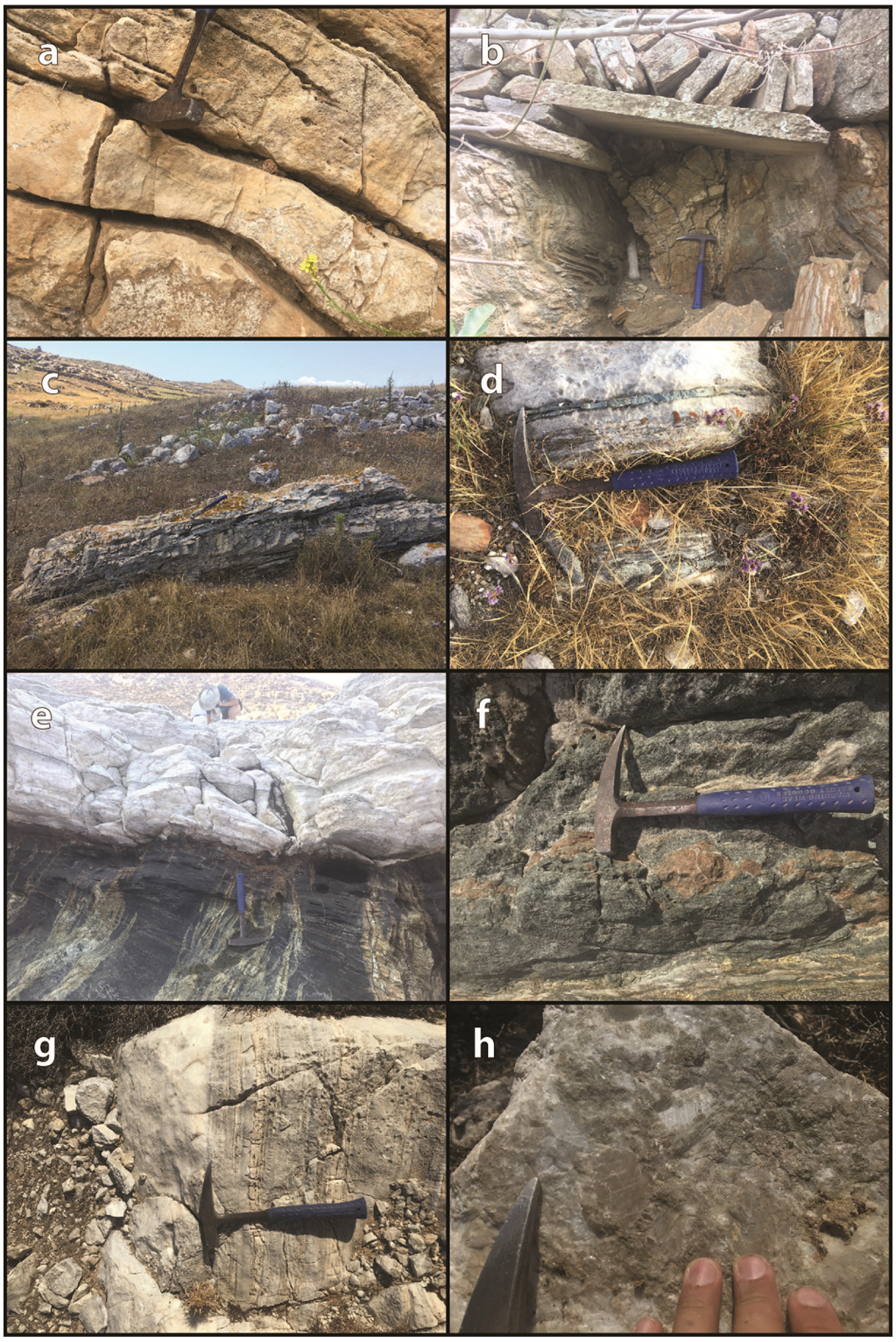

Fig. 4. (a) Calcitic marble boudinage inside the Inopos reservoir (C23); (b) Intense folding in the south of Inopos reservoir (C23). Marble and amphibolite reach a vertical dip; (c) Strongly fractured dolomitic marble in the northern part of Ghlastropi hill (C24); (d) Pyroxenite boudinage inside calcitic marble, Ghlastropi hill (C24); (e) Southern skarn between amphibolite and marble in quarry C25. Fine amphibolite foliation is perpendicularly cut by epidote veins; (f) Pyroxenite with decimetric garnet clusters in the northern skarn of quarry C25; (g) Thin whitish dolomitic layers inside C32 calcitic marble; (h) Calcitic marble with centimetre-size crystals, C32.

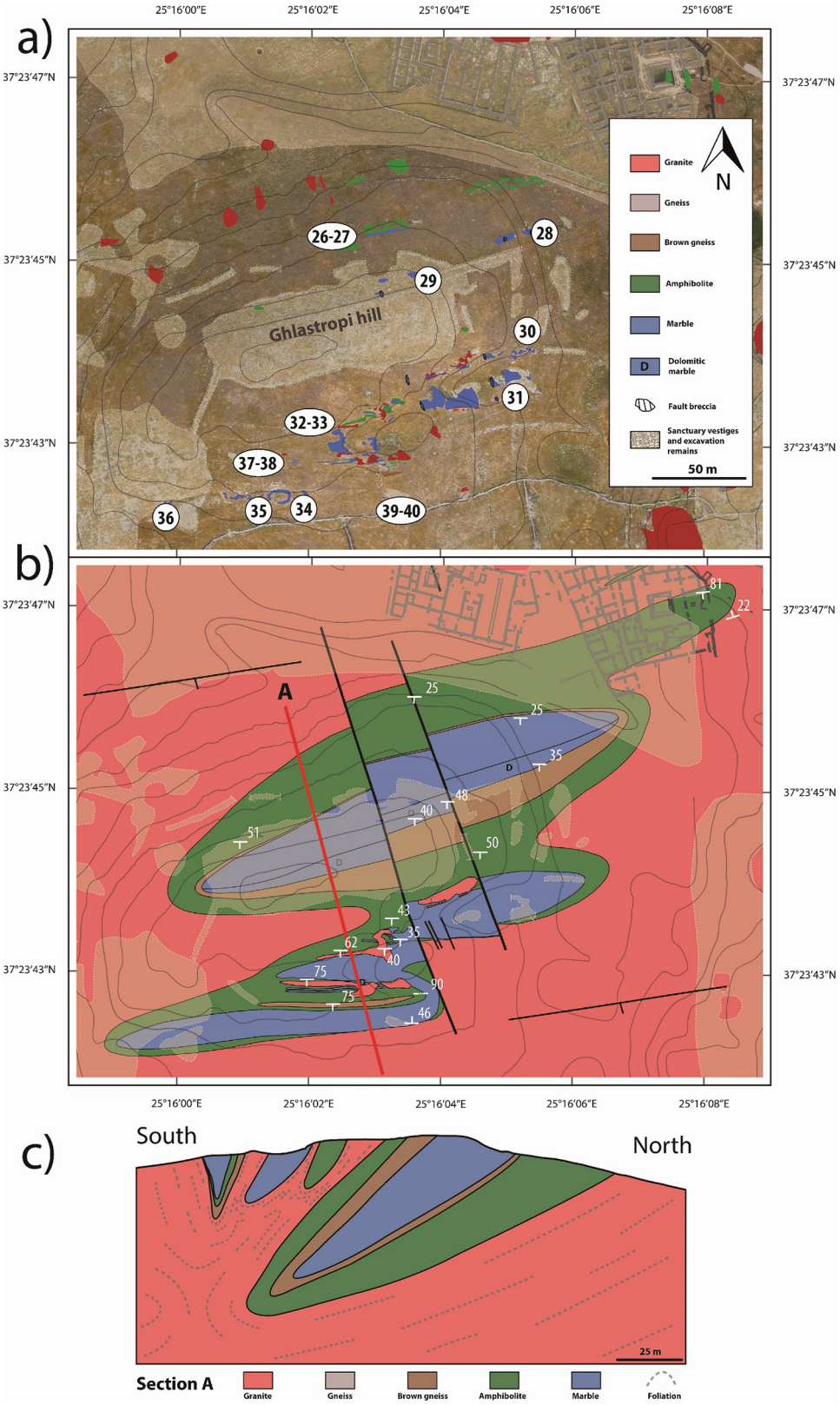

Fig. 5. (a) Location of the lithological outcrops and marble samples (n° 26 to n° 40) on the satellite map of the Ghlastropi hill quarry C24. The beige colour shows the areas covered by ruins or excavation debris, making the outcrops inaccessible; (b) 5000th scale geological map of the quarry C24. The red line locate the cross section A described below; (c) Cross section A located in quarry C24.

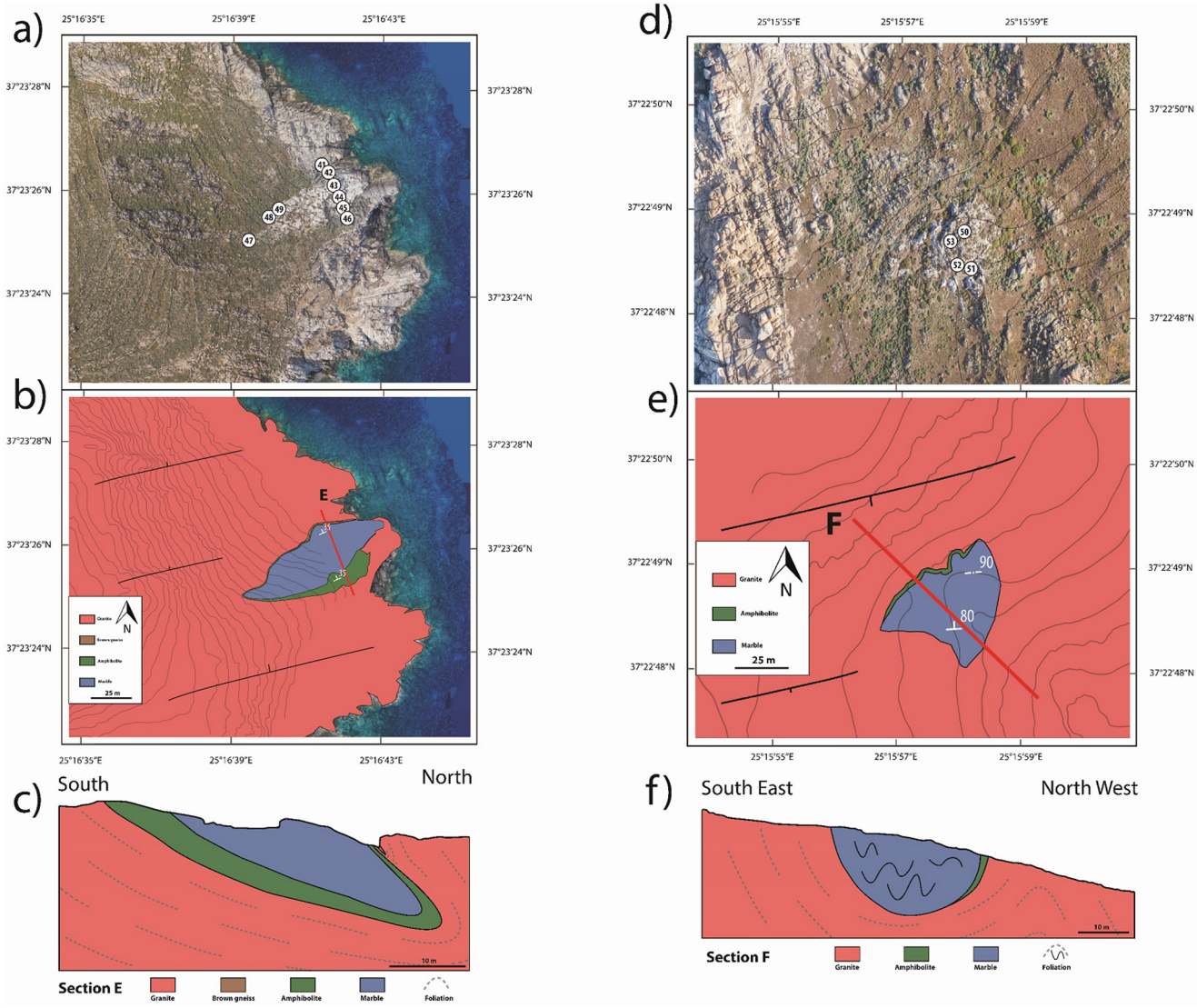

Fig. 6. (a,d) Location of marble samples on the satellite map of the quarry C25 (a, n° 41 to n° 49) and C32 (d, n° 50 to n° 53); (b,e) 5000th scale geological map of the quarry C25 (b) and quarry C32 (e). Red lines locate the two cross sections E and F. (c,f) Cross section E in quarry C25 (c) and F in quarry C32 (f).

The southern contact between marble and finely crystallised amphibolite is characterized by a centimetric reactional complex layer (Fig. 4e). It consists of a 5 cm thick layer of centimetric calcic garnets (andradite and grossular type) and diopside already identified by Cayeux (1911). Its thickness decreases towards the west and east, reaching a thickness of ten centimetres at the ends of the lens. The NE-SW foliation of the amphibolite which is parallel to the marble foliation and lens direction, is perpendicularly cut by epidote-rich veins associated with centimetric hedenbergite (Fig. 4e).

The northern contact between the marble lens and the granite laccolith is formed by a 3 m thick amphibolite-marble sequence. As observed previously, the amphibolite-marble contacts are underlain by a garnet-diopside skarn layer forming locally decimetric garnet clusters (Fig. 4f). The amphibolite is perpendicularly cut by epidote veins of smaller dimension compared to the southern ones.

Quarry C32 is located far from the previous ones in the southwest of the island, west of the hill Kato Vardia (Figs. 6d–6f). A boat landing was built below the quarry to facilitate the transport of granite blocks extracted from neighbouring quarries to the centre of the island where the majority of the buildings are located. Marble occurs in a 30 m long and 20 m large lens organised into two areas with no clear limits, in a vertical symmetrical synform. The entire quarry is highly fractured and the alternating marble layers are thin (between 10 cm and 1 m). The south-eastern part corresponds to a five meter thick layer of coarse pluri-millimetric marble whose colour alternates between dark blue and white. The north-western part corresponds to an alternation of fine white dolomitic layers (Fig. 4g), coarse white to greyish pluri-millimetric layers and very coarse white layers with pluri-centimetric grains (Fig. 4h). Marble layers dip 85 degrees to the north. There is a wide range of grain sizes in this lens with

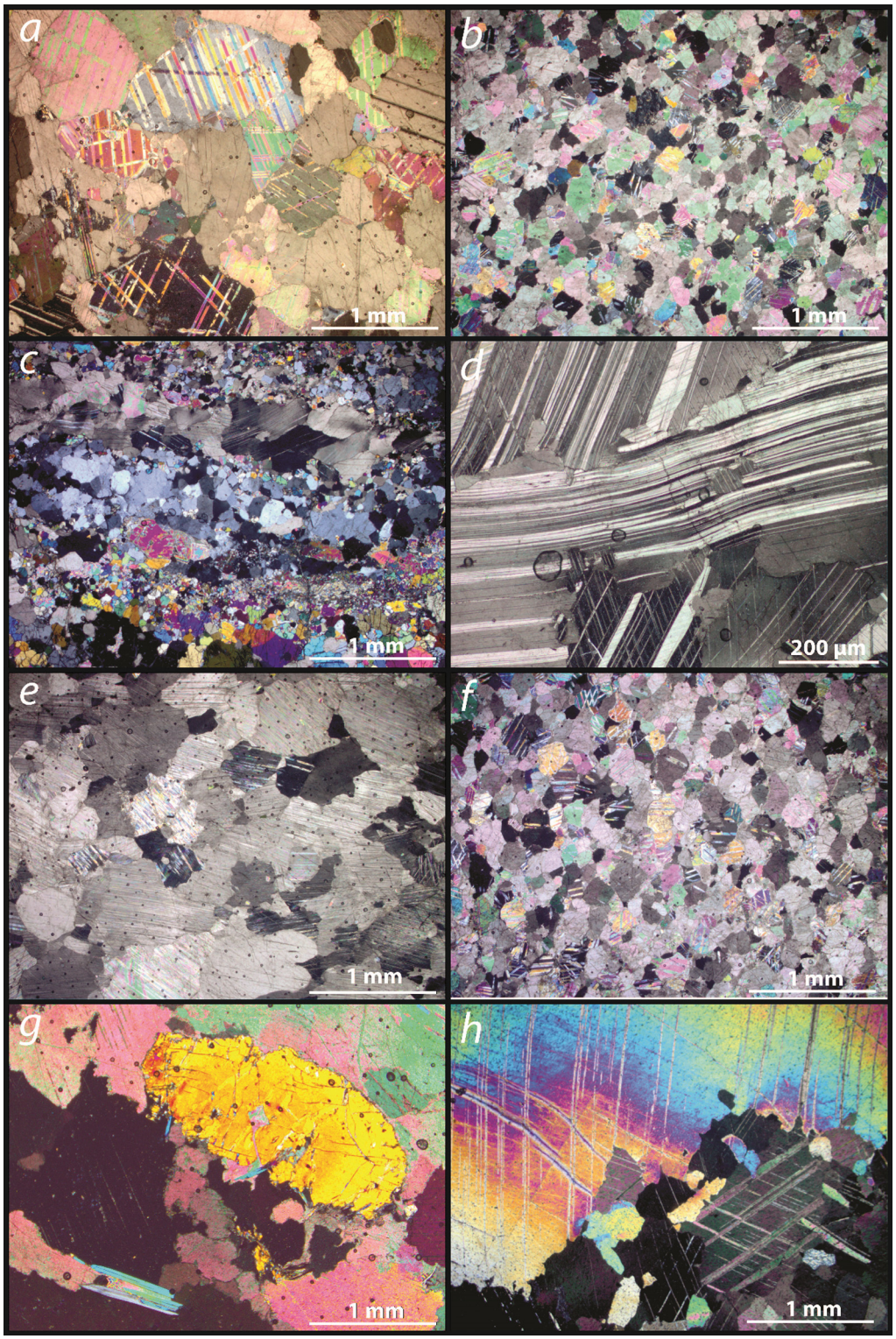

Fig. 7. Photomicrographs of thin sections of representative marbles from C23 (a, b, c, d) and C24 (e, f, g, h) observed in crossed polarized light. (a) calcitic marble from the centre of the theatre hill; (b) dolomitic marble from the western extremity of the main lens of the quarry; (c) calcitic marble sampled in the Inopos reservoir folding, in contact with amphibolite, showing a succession of calcite, quartz and pyroxene veins; (d) calcitic marble from the highly thinned part of the lens, eastern part of theatre hill, showing calcite cleavage folding; (e) calcitic marble from the northern lens of Ghlastropi hill quarry; (f) dolomitic marble from the northern lens of Ghlastropi hill quarry; (g) calcitic marble sampled in the core of the tight C24 fold, showing a large humite with fluorphlogopite and clinochlore; (h) calcitic marble from the southwestern part of the main Ghlastropi lens, showing a centimetre-size calcite crystal.

calcite/dolomite crystals measuring from 0.5 mm to several centimetres in diameter. The lens is in direct contact with the granite except its north-western limit which is marked by a thin amphibolite layer (10 cm).

3.2 Petrography and geochemistry

Marble samples were studied as a function of their exploitability in Delian architecture: the core of lenses where large blocks were excavated; intensely fractured areas where small bricks were extracted; strong ductile deformation zones and skarns, and poorly usable marbles (see Figs. 2a, 5a, 6a and 6d for sample location).

3.2.1 The Central quarry

The large lens of the central quarry C23 and the small neighbouring lenses show two types of marble: a white to greyish (N9 to 5B 7/1 in Munsell colour chart: Munsell, 1905) calcitic marble interbedded with a yellowish (between 5Y 8/1 and 10YR 8/6 in Munsell colour chart) dolomitic marble (Fig. 3c).

3.2.1.1 Lens core

Within the core of the lens, calcitic marble is a coarse heteroblastic (HE) marble with a maximum grain size ranging from 3.25 mm to 4 mm (Figs. 7a, 7c and 7d) compared to dolomitic marbles which are fine-grained (0.5 mm) homeoblastic (HO; Fig. 7b) marbles (Tab. 1). The fabric of calcitic marbles is essentially of mortar type, and mosaic dominates in dolomitic marbles. Calcite cleavages are not deformed for both types of marble. Crystal boundaries are interlobate throughout the core of the lens. The most abundant accessory minerals (Tab. 1) are phlogopite/fluorophlogopite (K–Fe–Mg bearing micas, up to 10%), quartz (up to 3%) and opaque minerals (mainly pyrrhotite and goethite). Phlogopite and opaques are present in both calcitic and dolomitic marbles while quartz is essentially present in calcitic marbles, associated with higher concentrations of phlogopite. Trace amounts of titanite, greenalite (serpentine-group mineral), clinochlore, diopside and spinel have been observed. Calcitic marble $\delta^{18}O$ signature shows a narrow range of values (−4.84% to −4.08‰) compared to dolomitic marble (−9.08% to −5.27‰). Carbon isotopic signature shows a small range of variation with higher values in calcitic marbles (1.67‰ to 2.31‰) compared to dolomitic marbles (−0.14‰ to 0.76‰).

3.2.1.2 Fractured zones

Fractured marble (Figs. 2a and 2c), shows the same grain size as previous marbles, with a MGS between 2 mm and 3 mm for calcitic marbles, and 0.5 mm for dolomitic ones (Tab. 1). Their fabric and accessory minerals are similar to the core of the lens. Trace amounts of clinochlore, anorthite, diopside, titanite and autunite were found. Fracturation seems to affect the oxygen isotopic signature in calcitic marble with a $\delta^{18}O$ showing lower values ranging from −9.08‰ to −8.17‰. This could be more likely due to the late interaction between marble and meteoric water (Herz, 1988). Dolomitic marble seem to be less affected by these interactions (−9.77‰ to −6.1‰ *versus* −9.08‰ to −5.27‰ in the core of the lens). The $\delta^{13}C$ isotopic signature (Fig. 8a) shows the same range of variation as in the non-fractured zones (0.2‰ to 1.25‰, Tab. 1).

3.2.1.3 Intense ductile deformation areas

Both calcitic and dolomitic marbles are heteroblastic with mortar fabric and interlobate to amoeboid crystal boundaries. Calcite and dolomite grains often show internal grain deformation (folded cleavages; Figs. 7c and 7d) as well as vein mineralisations (Tab. 1).

Marbles located in thinned boudinaged outcrops show large amounts of quartz and phlogopite in thin folded layers at geological contacts (up to 10%, Tab. 1). Other mineral phases appear occasionally such as diopside, clinochlore, titanite, anorthite, zircon, talc, scheelite, autunite and thorite. The oxygen isotopic signature shows a large range of low values for calcitic marble (−18.83‰ to −4.47‰) and a very short interval of values for dolomitic marble (−12.3‰ to −11.3‰, Tab. 1). $\delta^{13}C$ isotopic signatures range within the same interval (−0.58‰ to 2.05‰) observed throughout the lens. The drop in $\delta^{18}O$ values could be related to interactions with calc-silicate minerals such as diopside at high temperatures during folding (Shieh and Taylor, 1969).

3.2.2 The Ghlastropi hill quarry

The two lenses of the Ghlastropi hill quarry C24 show an interbedding of marble layers similar to observed in C23, *i.e.*, a calcitic marble of white, orange and bluish colour (Figs. 3f and 7e, respectively N9, 10YR 8/6 and 5B 7/1 in Munsell colour chart: Munsell, 1905) and an orange dolomitic marble (Fig. 7f, between 5Y 8/1 and 10YR 8/6 in Munsell colour chart).

3.2.2.1 The excavated lenses core

Calcitic marble is medium coarse grained and heteroblastic with a maximum grain size ranging from 1.5 to 4 mm; dolomitic marble is fine-grained and homeoblastic (MGS = 0.5 mm; Tab. 1). Mortar fabric dominates in calcitic marbles while mosaic fabric occurs in dolomitic marbles. Calcite and dolomite crystal boundaries are mostly interlobate throughout the lens.

Quartz is less abundant in C24 than in C23, not exceeding 1%. Opaque minerals (pyrrhotite and goethite) and phlogopite are widespread, varying from 0.5% to 2.6% (Tab. 1). The isotopic signature of $\delta^{18}O$ and $\delta^{13}C$ are similar to those of quarry C23, ranging respectively from −7.24‰ to −1.81‰ and 0.1‰ to 2.47‰ (Tab. 1, Fig. 8b).

3.2.2.2 The fractured zone

Apart from surface fracturing, the fabric and texture are virtually the same as those encountered in the excavated lens core. Beside phlogopite and quartz, minute amounts of accessory minerals such as titanite and Mg-chlorite are observed (Tab. 1). As observed in quarry C23, the highly fractured part of the marble shows more negative $\delta^{18}O$ values (−9.58‰; −8.55‰; Tab. 1). The $\delta^{13}C$ signature remains in the same range as the previous marbles (0.74‰; 0.76‰).

Table 1. Results of the petrographic and isotopic analyses of the four Delian marble quarries.

Marble quarry	Area	Sample	MGS (mm)	Grain repartition	Fabric	Internal grain deformation	Lineations	Fractures	Crystal boundaries	Dolomite (XRD)	Quartz (Microscope, XRD)	Phlogopites (Microscope, XRD)	Opaques	Other mineral (XRD, SEM-EDS)	$\delta^{13}C$	$\delta^{13}C$ DEV	$\delta^{18}O$	$\delta^{18}O$ DEV
C23	Lens core	4	0.5	HO	Mosaïc	No	No	No	Interlobate	91.9%	+	++	+	Serp	−0.15	0.29	−5.27	0.25
		6	0.5	HO	Mosaïc	No	Yes	No	Interlobate	87.8%	++	++	+−	Tit	0.76	0.06	−8.32	0.53
		8	0.5	HO	Mosaïc	No	No	No	Interlobate	84.7%	+	+	−		−0.14	0.43	−9.08	0.23
		5	4	HE	Mosaïc	No	No	No	Interlobate	–	+	++	+	Dio, Cli, Serp, Spi	2.31	0.25	−4.08	0.39
		7	3.25	HE	Mortar	No	No	No	Interlobate	1.5%	+++	+++	+−		2.25	0.18	−4.84	0.06
		9	3.75	HE	Mortar	No	Yes	Yes	Polygonal	–	+	−	+−		1.67	0.14	−4.69	0.16
C23	Intensely fractured	2	0.5	HO	Mosaïc	No	No	No	Interlobate	90.8%	−	+	+	Tit	0.65	0.23	−8.18	0.86
		3	0.5	HO	Mosaïc	No	No	Yes	Interlobate	92.2%	−	++	+		1.25	0.04	−9.77	0.23
		10	0.5	HO	Mosaïc	No	No	No	Interlobate	88.4%	+	++	+−		0.20	0.45	−6.10	0.69
		1	3	HE	Mortar	No	No	Yes	Amoeboid	27.7%	+	++	+++	Cli, Ano	1.16	0.18	−8.17	1.39
		11	2	HE	Mortar	No	Yes	Yes	Amoeboid	–	++	+++	++	Dio, Aut	0.87	0.40	−9.08	0.29
C23	Strong ductile deformation	17	0.5	HE	Mortar	No	Yes	Yes	Amoeboid	95.0%	−	+	+	Tit	0.00	0.22	−11.94	0.58
		19	0.5	HE	Mortar	No	No	No	Interlobate	97.1%	−	−	++		0.35	0.01	−12.30	0.12
		24	0.5	HE	Mortar	No	No	No	Interlobate	94.8%	−	+	+−	Tit, Cli, Ano	0.86	0.09	−11.32	0.29
		12	2.5	HE	Mosaïc	Yes	No	Yes	Interlobate	0.8%	+	−	+−		−0.33	1.19	−8.99	0.39
		13	2	HE	Mortar	Yes	No	Yes	Interlobate	–	−	+	+−		0.43	0.14	−4.47	0.25
		14	3.5	HE	Mortar	Yes	Yes	Yes	Amoeboid	1.2%	+	+	+−	Dio, Talc	1.01	0.43	−18.83	1.44
		15	3	HE	Mortar	Yes	Yes	Yes	Amoeboid	–	+	−	+−	Sch, Feld	1.14	0.14	−15.12	0.29
		16	3	HE	Mortar	Yes	Yes	Yes	Amoeboid	–	+++	+++	+−	Dio, Cli	0.31	0.01	−14.79	0.17
		18	3							–	+++	+++			−0.52	0.46	−15.23	0.07
		20	2.25							–	+++	+++		Zir	1.34	0.04	−15.48	0.34
		21	1.5	HE	Mortar	No	No	No	Amoeboid	0.5%	+	++	+−	Cli	−0.65	0.01	−14.92	0.06
		22	0.8	HE	Mosaïc	Yes	Yes	Yes	Polygonal	0.5%	+	++	+++	Tit, Dio, Ano, Cli, Aut, Thor, Zir, Feld, Epid	−0.58	0.16	−14.42	0.20
		23	2	HE	Mortar	Yes	Yes	Yes	Amoeboid	–	++	+	++		2.01	0.17	−12.41	0.09
		25	4	HE	Mortar	No	Yes	Yes	Amoeboid	–	+	++	++	Dio, Ano	2.05	0.36	−6.60	0.66
C24	Lens core	30	1							–	−	+			0.10	0.23	−6.41	0.18
		31	2.5	HE	Mortar	Yes	No	Yes	Interlobate	–	+	−	+−	Dio	1.55	0.19	−6.67	0.06
		32	3	HE	Mortar	No	No	Yes	Amoeboid	–	−	+++	++	Cli	2.32	0.01	−2.40	0.05
		33	3	HE	Mortar	No	No	Yes	Amoeboid	–	+	+++	++		2.47	0.19	−1.81	0.03
		34	4	HE	Mosaïc	No	No	No	Interlobate	–	−	+	−	Dio	1.79	0.03	−6.69	0.01
		35	> 20	HE	Mortar	No	Yes	No	Interlobate	–	−	−	−		1.72	0.21	−7.24	0.24
		36	4	HE	Mosaïc	No	No	Yes	Interlobate	–	−	−	−		0.48	0.10	−3.15	0.06
C24	Intensely fractured	28	0.5	HE	Mosaïc	No	No	No	Interlobate	94.6%	−	+	+	Tit	0.76	0.21	−8.55	0.07
		29	0.5	HE	Mosaïc	No	No	Yes	Interlobate	89.6%	−	+++	+−	Cli	0.74	0.22	−9.58	1.98

Table 1. (continued).

Marble quarry	Area	Sample	MGS (mm)	Grain repartition	Fabric	Internal grain deformation	Lineations	Fractures	Crystal boundaries	Dolomite (XRD)	Quartz (Microscope, XRD)	Phlogopites (Microscope, XRD)	Opaques	Other mineral (XRD, SEM-EDS)	$\delta^{13}C$	$\delta^{13}C$ DEV	$\delta^{18}O$	$\delta^{18}O$ DEV
C24	Strong ductile deformation	26	1.5	HE	Mortar	Yes	No	Yes	Interlobate	–	+	+	++		2.06	0.16	−11.52	0.29
		27	1.5	HE	Mortar	Yes	No	No	Interlobate	–	–	++	+−		0.13	0.19	−5.01	0.20
		37	3	HE	Mortar	No	Yes	Yes	Amoeboid	–	+	+	+−	Dio, Hum, Spi, Amp, Tour	1.79	0.00	−13.85	0.21
		38	3	HE	Mortar	No	Yes	Yes	Amoeboid	1.9%	++	+++	+−	Cli	1.25	0.05	−13.25	0.13
		39	> 20	HE	Mortar	Yes	No	Yes	Interlobate				–					
		40	3	HE	Mortar	Yes	Yes	Yes	Interlobate	–	+	+	+−	Dio, Grn	1.54	0.25	−11.87	2.93
C25	Lens core	41	> 20	HE	Mortar	No	Yes	No	Interlobate	–	+++	+++	+++		2.68	0.04	−5.63	0.52
		42	> 20	HE	Mortar	No	Yes	No	Interlobate	–	–	+	–		2.73	0.01	−7.77	0.04
		43	> 20	HE	Mortar	No	Yes	Yes	Amoeboid	–	–	–	++		2.77	0.02	−5.59	0.15
		44	> 20	HE	Mortar	Yes	Yes	Yes	Amoeboid	–	–	–	++		2.49	0.04	−11.04	0.27
		45	> 20	HE	Mortar	No	No	Yes	Amoeboid	–	–	–	–		2.86	0.03	−6.45	0.20
		46	2.5	HE	Mortar	No	Yes	Yes	Amoeboid	–	–	–	+−		2.93	0.03	−5.63	0.04
		47	> 20												2.71	0.03	−6.30	0.05
		48	> 20												2.61	0.03	−8.45	0.08
C25	Skarn	49	> 20												1.80	0.47	−10.90	1.82
C32	Lens core	50	1	HE	Mortar	No	Yes	No	Amoeboid	87.3%	–	+	+−	Tit	1.39	0.12	−7.37	0.46
		51	3.5	HE	Mortar	No	No	No	Amoeboid	–	+	++	+−	Ano	3.18	0.09	−2.63	0.08
		52	5	HE	Mortar	No	No	No	Amoeboid	1.2%	+	++	–		1.89	0.15	−5.69	1.48
		53	12	HE	Mortar	No	No	No	Amoeboid	–	+	+	+++		2.52	0.04	−2.96	0.04

HE: heteroblastic; HO: homeoblastic; +++: very abundant; ++: abundant; +: present; + −: traces; −: absence; Amp: amphibole; Ano: anorthite; Aut: autunite (uranium secondary mineral); Cli: clinochlore; Dio: diopside; Epid: epidote (Ce–La–allanite); Feld: feldspath; Grn: garnet (calcic garnet: andradite–grossular); Hum: humite; Sch: scheelite ($CaWO_4$); Serp: greenalite (serpentine group mineral); Spi: spinel; Talc: talc; Thor: thorite (thorium analogue of zircon); Tit: titanite; Tour: tourmaline; Zir: zircon. DEV is the standard deviation of $\delta^{18}O$ and $\delta^{13}C$ measurements.

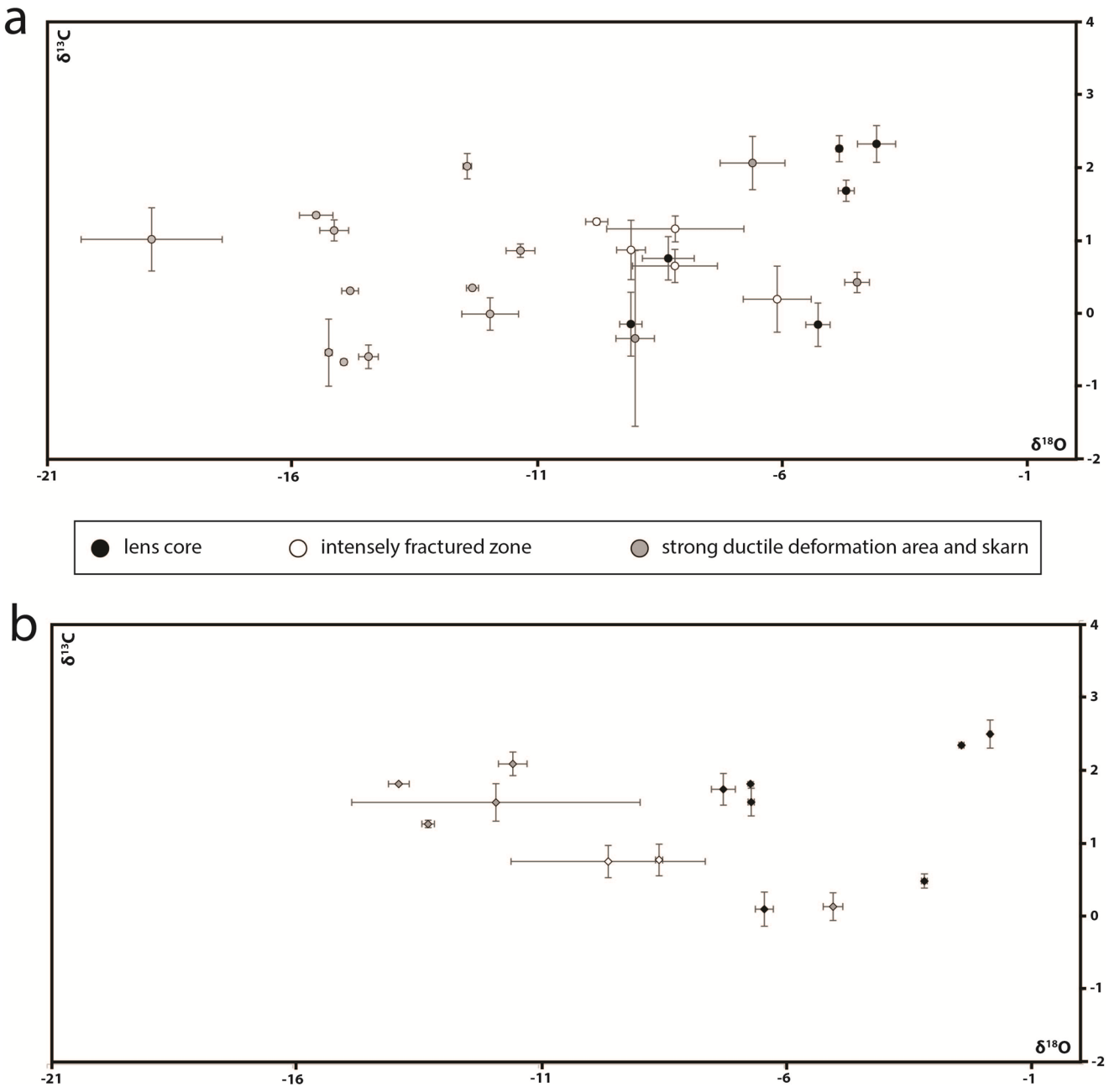

Fig. 8. Carbon isotopic signature *versus* oxygen isotopic signature in quarry C23 (a) and quarry C24 (b). Blue colour corresponds to the core of the lenses, yellow colour corresponds to highly fractures areas and red colour to folded/thinned zones and skarns.

3.2.2.3 Strong ductile deformation areas and skarns

Marbles sampled in the tight southern fold, near marble-amphibolite contacts and at the southern skarn correspond to heteroblastic calcitic marbles with mortar fabric (Fig. 7h). Their crystal boundaries are interlobate and amoeboid. Their calcite grains form lineations and show fracturation. Marble in the centre of the tight fold incorporates pyroxenite boudins (Fig. 4d) and all minerals (calcite, pyroxenes and other accessory minerals) are crystallized in veins and are enriched in quartz (1%) and phlogopite (up to 10%). The marble close to the southern skarn, at the granite contact, shows an increase of calcite crystal size from 3 mm (MGS = 3 mm) to pluri-centimetric (up to 40 mm). This grain size gradient is evidence for a thermal gradient towards the contact with enclosing granite while the rest of the marble lenses are isolated from this thermal effect by the amphibolite layer (Fig. 7h). Diopside, quartz, phlogopite and grossular/andradite type garnets are visible in the marble close to the skarn. In the thinned part of the fold, one finds Mg chlorite and humite associated with diopside and spinel (Fig. 7g). These secondary OH-bearing minerals may result from hydration of a diopside-rich layer.

As for C23, $\delta^{18}O$ of the samples taken from folded and reaction zones has more negative values ranging from −14‰

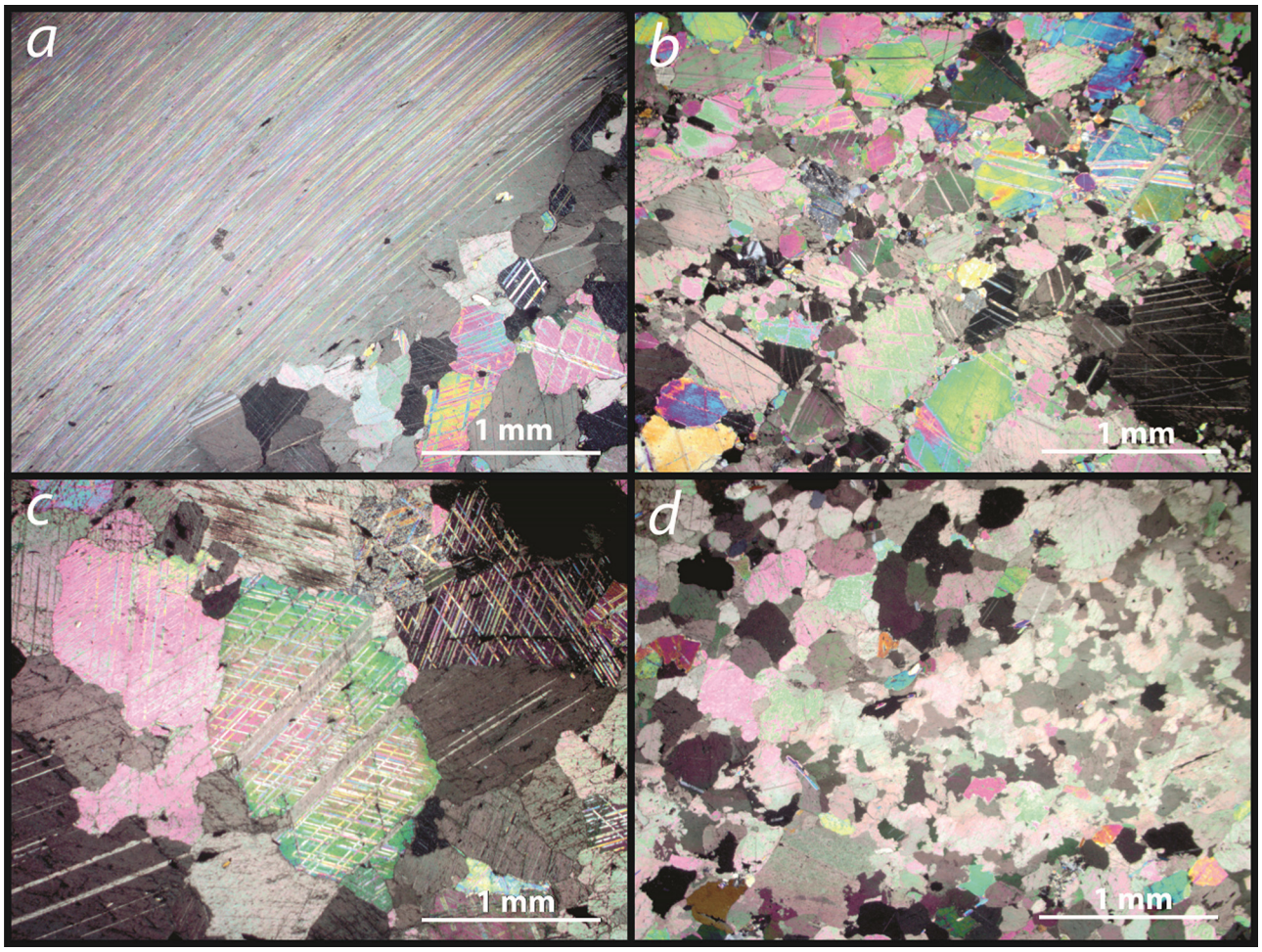

Fig. 9. Photomicrographs of thin sections of representative marbles from C25 (a, b) and C32 (c, d) observed in crossed polarized light. (a) main calcitic marble of quarry C25, showing centimetre-size crystals; (b) calcitic marble from the southern contact of C25 lens showing multiple calcite lineations; (c) calcitic marble from quarry C32; (d) dolomitic marble from quarry C32.

to −11‰ while $\delta^{13}C$ remains in the same range (between 0.13‰ and 2.06‰, Tab. 1).

3.2.3 The southernmost and easternmost quarries

Quarry C25, located southeast of Mount Cynthus, and Quarry C32, located south of the island on the west coast, both consist of a single lens but are very different texturally and mineralogically. Quarry C25 consists exclusively of calcitic marble (Fig. 6a). Quarry C32 consists of an alternation of calcitic and dolomitic layers (Fig. 6d).

3.2.3.1 Quarry C25

Marble from C25 is heteroblastic to porphyroblastic with spectacular pluri-centimetric grains (up to 60 mm, *i.e.*, giant grained) white to dark blue (Fig. 9a, N9 to 5PB 3/2 in Munsell colour chart, Munsell, 1905) calcite crystals showing strong polysynthetic twinning. Its fabric is mortar type. There is almost no deformation in calcite cleavages, however fractures and mineralized veins of calcite are common (Fig. 9b). Calcite crystal boundaries are interlobate in the northern skarn of the lens and amoeboid in the rest of the lens.

Marbles from quarry C25 are relatively poor in accessory minerals except for marble in contact with the northern skarn of the lens which does contain F-phlogopite (up to 10%), quartz (almost 2%) and opaque minerals (pyrrhotite and goethite). Thin dark layers of small garnets can be found near the southern contact between the marble and the amphibolite isolating the marble lens from granite. $\delta^{13}C$ shows higher values compared to previous quarries and a very narrow range of variation (2.49‰ to 2.93‰). The sample taken in the north-west of the lens at the marble-amphibolite contact, is an exception with a value of 1.8‰. The carbon isotope content is homogeneous throughout the quarry while $\delta^{18}O$ ranges from −11.04‰ to −5.59‰ (Fig. 10, Tab. 1).

3.2.3.2 Quarry C32

Marble from C32 can be divided into three categories as in quarry C24. The lens contains a whitish to bluish (N9 to 5B 7/1 in Munsell colour chart) coarse calcitic marble, a pure white

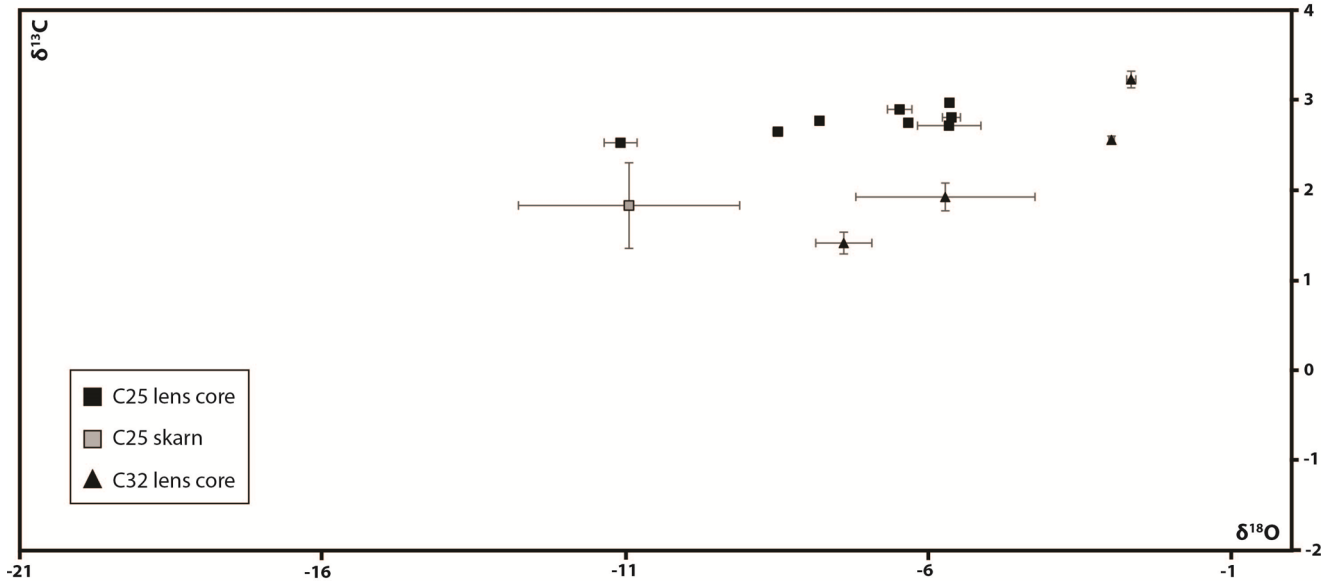

Fig. 10. Carbon isotopic signature *versus* oxygen isotopic signature in quarry C25 (squares) and quarry C32 (triangles).

(N9 in Munsell colour chart) dolomitic marble and a whitish (N9 to N8 in Munsell colour chart) centimetric marble (Fig. 4h). All three are heteroblastic marbles of mortar type fabric with amoeboid crystal boundaries (Figs. 9c and 9d). They show no deformation or fractures in the calcite/dolomite cleavages. Only the dolomitic part of C32 shows mineralized veins of calcite. Quartz is rather scarce (around 0.5%). Phlogopite grains are observed throughout the lens. Opaque minerals (pyrrhotite and goethite) are rare in this quarry, except in the pluri-centimetric marble (Tab. 1) where they are numerous. Some titanite and anorthite are also visible. The dolomitic layers in this quarry contains less dolomite than in the previous quarries. This could be due to dedolomitization as suggested by Hadjidakis *et al.* (2003). The $\delta^{18}O$ isotopic signature of C32 samples varies between −7.4‰ and −2.6‰, $\delta^{13}C$ signature fluctuates from 1.4‰ to 3.2‰ (Tab. 1). Despite the small size of quarry C32, its carbon and oxygen content varies greatly within marble layering, reflecting heterogeneities throughout the quarry.

4 Discussion

The geological map of marble quarries C23 (Fig. 2b) and C24 (Fig. 5b) at smaller scale (1/5000) than previous studies (1/10 000: Cayeux, 1911; Jolivet *et al.*, 2021) was largely modified compared to Cayeux (1911) with further details on the lithological contacts. Note that these two quarries are partly covered by ruins, being located within the ancient town. Therefore, they are subjected to different geological interpretations related to variable appreciations of lithological contacts, fault breccias and mineralization. Heteroblastic fabric, mortar texture and curved grain boundaries, which are typical of calcitic marble, record synkinematic marble deformation as the granite lacothith was intruding the metamorphic sequence (marble, amphibolite, brown gneiss for the Cycladic Blueschist Unit). Medium to coarse MGS of calcite crystals are evidence for high-grade amphibolite facies metamorphism when the Mykonos–Delos–Rhenia MCC was exhumed as a HT dome (see Sect. 1.2 and Jolivet *et al.*, 2015, 2021). The finer-grained dolomitic layers showing homeoblastic fabric, do not record this event for mechanical reasons, dolomite being stronger than calcite at this temperature (Kushnir *et al.*, 2015; Berger *et al.*, 2016). Anhydrous progressive metamorphic assemblages in marble (calcite, dolomite, diopside, grossular, spinel) and adjacent calc-silicate rocks (diopside–anorthite–calcite quartz) retrograded to hydrous mineral assemblage such as clinochlore, F-phlogopite, humite with decreasing temperature and increasing water activity. This rehydration of the rocks may be related to late stages of volatiles-rich granite emplacement.

The new mapping of marble quarries modifies the volume estimation of excavated material. (Fig. 11). Cayeux (1911) interpreted quarry C23 as five small marble lenses less than 30 m long: three lenses in a large enclave of brown gneiss within the theatre hill separated from the other two by the Inopos stream. In the new geological map proposed in this paper (Fig. 2b), quarry C23 consists of a large marble lens oriented NE-SW, cut by a N-S fault at the Inopos stream. This 200 m long lens was massively exploited around the theatre hill, but also behind the theatre and in the Inopos reservoir. The surface area of this lens was thus revised from 1360 m^2 to 3410 m^2, which greatly increases the quantity of potentially extracted marble. The surface area of the C24 marble has also been significantly increased from 700 m^2 to 4400 m^2. The outline of the northern lens drawn by Cayeux (1911; Fig. 11) is significantly enlarged to a new 170 m length (Fig. 5b). The three southern lenses proposed by Cayeux (1911) at Ghlastropi are reinterpreted as a single, strongly folded lens of 260 m length.

The geological map of quarries C25 and C32 has not been modified (Figs. 6b–6e) from the study of Cayeux (1911). The marble and its various geological contacts outcrops are perfectly visible so there is no ambiguity about the location of geological contacts.

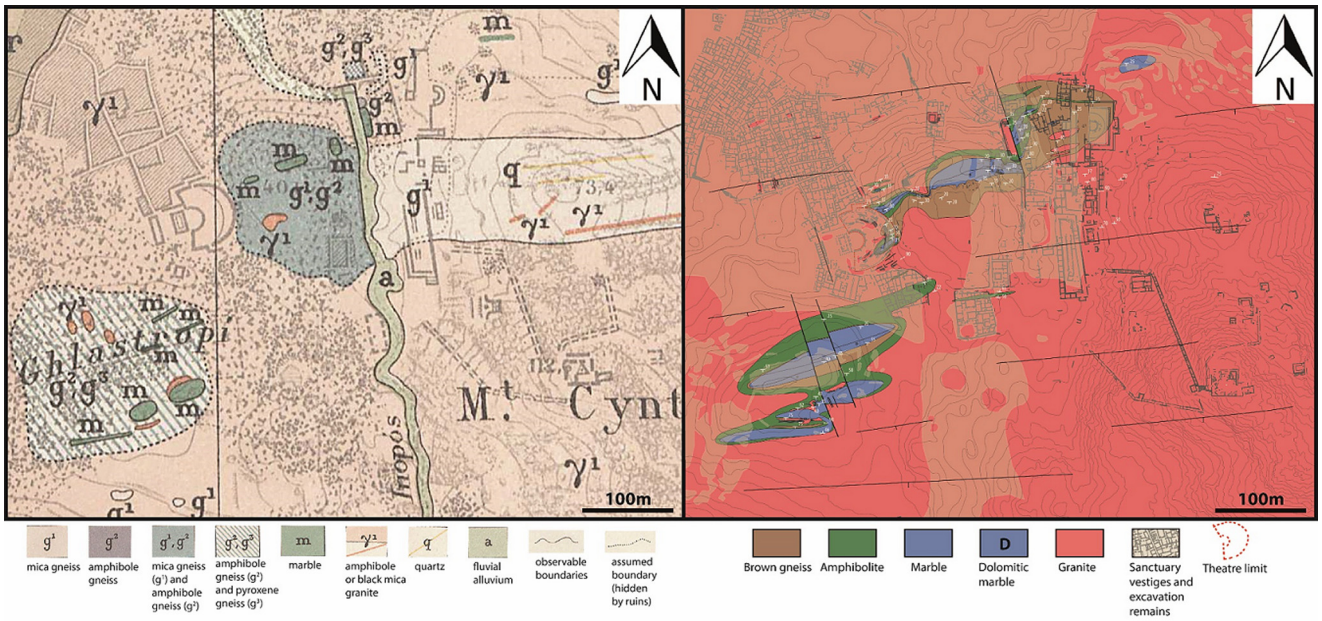

Fig. 11. (a) 10 000th scale geological map of the two main marble quarries C23 (central quarry) and C24 (Ghlastropi quarry) proposed by Cayeux (1911); (b) New 5000th scale geological map of C23 and C24 quarries. The beige colour shows the areas covered by ruins or excavation debris, making the outcrops inaccessible.

The revision of extracted volumes in the two main quarries C23 and C24 invites to re-evaluate the volume of indigenous marble present in the ancient buildings.

The 220 m long main lens of C23 allowing extraction of a large volume of marble despite its deformations (fracturing, folding), has been quarried in almost its entire length. The main extraction zone located in the theatre hill allowed the extraction of large architectural blocks due to its limited deformation (Fig. 2a, n° 4 to n° 9). The fractured western and eastern ends (Fig. 3c) of the lens (Fig. 2a, n° 1-2-3-10-11) did not allow such a production, but nonetheless provide smaller blocks. The fine yellow to orange coloured dolomitic marble is easily macroscopically recognisable in ancient constructions (Figs. 3c–3e). Only the strongly folded zones were not excavated (Fig. 2a, n° 12 to n° 25). Most of the material appears to have been used in buildings adjacent to the extraction sites. For example, the fine yellowish dolomitic marble associated with dark green amphibolite extracted from the Inopos reservoir were used directly in the surrounding buildings, as shown within the walls in the Inopos district (Figs. 3b–3e).

As for C23, a large volume of marble was extracted from the Ghlastropi hill (C24, Fig. 5; 10). The extent of extraction is hard to determine in the northern lens as it is difficult to estimate the initial geological outcrop before excavation. However, the topography of the 180 m long southern lens is clearly cut to a depth of at least 4 m. It is within this second lens that most of the marble was extracted. The core of the lens, which is not intensely fractured, could have provided large architectural pieces that are thought to be found in the site (Figs. 3g and 3h). The southern part of the lens, although different from the rest of the quarry with its marble with centimetric calcite crystals, has been exploited. Indeed, this less massive part of the lens has provided numerous rubble stones that can easily be recognised in the surrounding ruins.

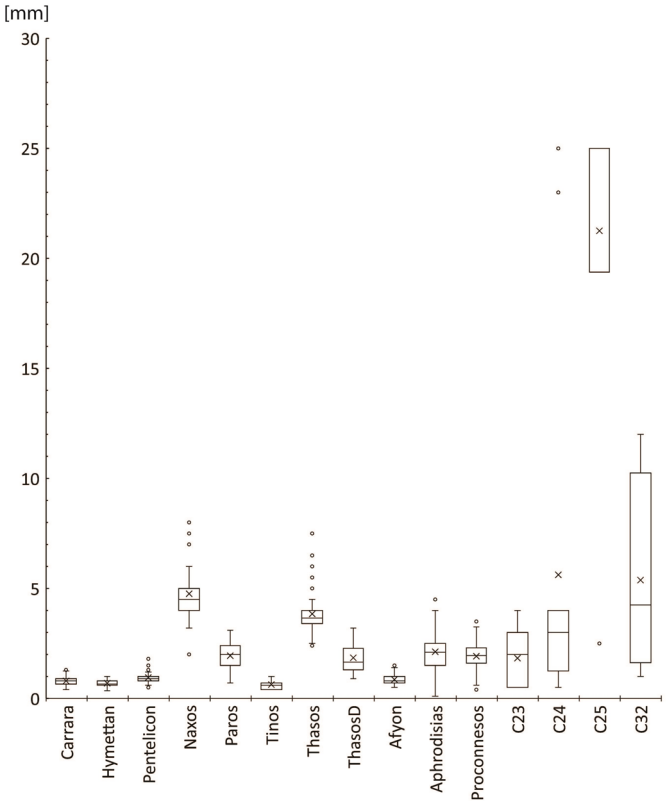

Fig. 12. Maximum Grain Size (MGS) of the most important marbles used in Antiquity. Values are in mm. Mean, median, 25th and 75th percentiles, minimum and maximum values are represented respectively by a cross, a central line, box limits, and whiskers. Consequently, boxes constitute a 50% clustering of MGS data. Circles correspond to outsider values.

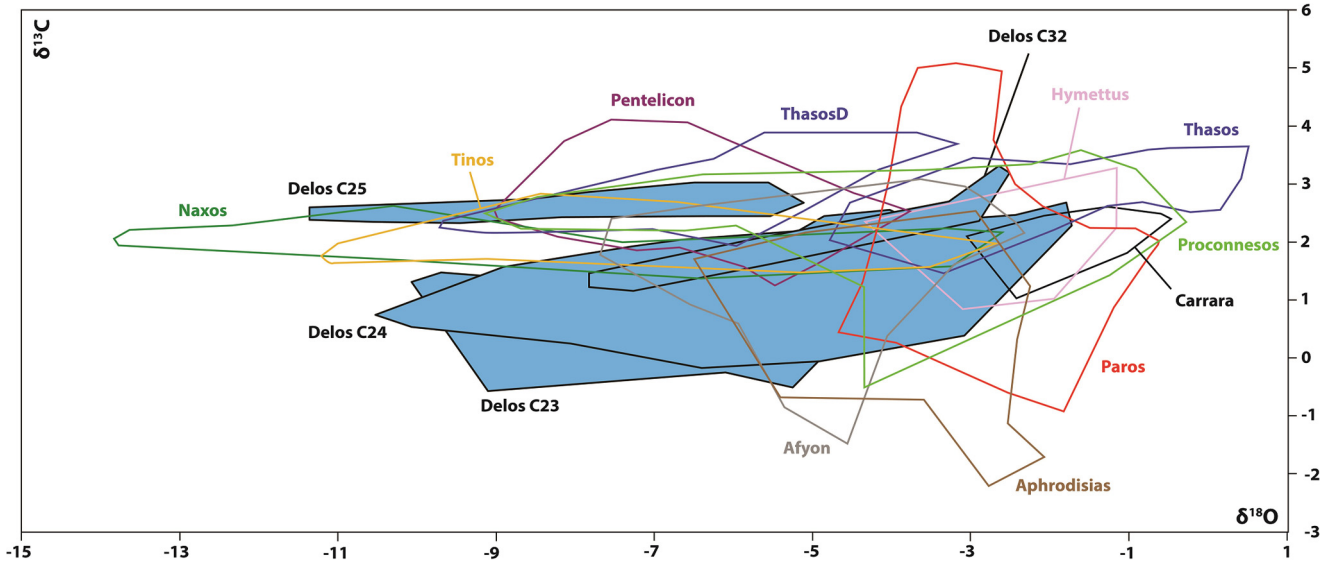

Fig. 13. Carbon isotopic signature *versus* oxygen isotopic signature of the four Delian marble quarries (blue colour: C23, C24, C25, C32) and the most important marbles used during Antiquity.

The topography of quarry C25 shows relics of metric block extraction (Fraisse and Kozelj, 1991). The exceptional characteristics of this marble with its giant whitish and bluish crystals make it easily macroscopically recognisable. Indeed marble C25 has been identified in many Delian buildings such as the Delta edifice, the second Heraion and the krepidoma of the temple of Apollo (Fraisse and Kozelj, 1991). However small volumes of a similar marble were identified in Quarries C24 and C32, which calls the macroscopic identification into question. Such provenances can be verified with isotopic analyses of carbon and oxygen composition which discriminate perfectly quarry C25 from the other Delian quarries.

In C32, the minor thickness of marbles layers and their high fracturation make the material very difficult to use in architecture. In contrast to quarries C23 and C24, the topography of this small quarry is not significantly indented, suggesting a small volume of extraction. It is therefore unlikely that large volumes of rock have been extracted from this quarry during Antiquity; they only quarried small blocks for use in shepherd's walls.

To summarize, the main quarries C23 and C24 provided a great quantity of marbles hard to identify by the naked eye, requiring micro-petrography and geochemical analysis. C25 as well as the south lens of C24 produced macroscopically identifiable blocks (as mentioned above). Topography relief and extraction marks suggest a poor excavation of quarry C32.

Several buildings dating back to the independence of Delos (in the theatre and its district, Ekklesasterion, Hyppostyle room, Aphrodision, Inopos district) were built with a marble with bluish to orange veining similar to the indigenous calcitic marble of C23 and C24 (Figs. 3f–3h). A provenance investigation of these edifices is required to confirm such a hypothesis.

The MGS analysis showed that C23, C24 Delian marbles are mainly medium to coarse grained with very fine dolomitic layers (Fig. 12). This high MGS due to the geological context of the island of Delos (a high temperature metamorphic core complex dome, Altherr and Siebel, 2002; Rabillard, 2017; Jolivet *et al.*, 2021) is a powerful tool to distinguish the Delian marbles among the marbles of the Mediterranean basin excluding fine-grained low grade marbles such as Pentelic, Hymettus and Tinos. Marbles similar to the Delian ones in terms of MGS are those of Paros, Naxos, Thasos (both the dolomitic marble Thasos and the calcitic one), Aphrodosias and Proconnesos.

Mineralogical analyses will provide little clue in the provenance studies as the accessory minerals present in Delian marbles are mainly quartz, phlogopite and iron oxides/sulphides, and common minerals in marbles. However, the calcite/dolomite ratio is a key parameter which quantifies the dolomite content of the marble, it can for example distinguish the calcitic Delian marble from the dolomitic marble of Thasos.

Although, the $\delta^{18}O$ isotopic signature of the Delian marbles shows a wide spread (Fig. 13), overlapping domains characteristic of a great variety of Mediterranean marbles, some outliers may be identified. It is possible to distinguish Delos from most of Paros quarries. However some of the Delian marbles have isotopic ratios equivalent to those of Marathi (Paros) with a $\delta^{18}O$ between −4.5‰ and −2‰. This same range of values also corresponds to the marbles of Aphrodisias, Proconnesos, and a part of Naxos (Melanes) and Thasos marbles. The MGS-isotope ratio approach should be completed by other techniques such as destructive or non-destructive elemental analyses, coupled with statistical Principal Component Analyses (PCA, Vettor *et al.*, 2021). Indeed, the study of strontium and rare earth elements in calcite can be discriminatory (Green *et al.*, 2002; Attanasio *et al.*, 2015; Poretti, 2016; Poretti *et al.*, 2017). Preliminary elemental analyses have already been carried out on the Delian marbles in a recent non-destructive marble provenance study (Vettor *et al.*, 2021).

5 Conclusion

This new mapping of Delian marble quarries brought major changes to the contours of quarries near the archaeological site (C23, C24). New marble outcrops were found allowing a reassessment of marble lenses dimensions (length and surface) thus a revision of the extracted marble volume in the island.

The marble quarry C32 located in the south-western part of Delos might have provided only a very limited volume of marble despite being nearby a boat landing. It is due to the small dimension of the outcrop, its strong fracturing and the poor thickness of its marble layers.

Part of marble production located away from the site, to the south east of Mount Cynthus (C25), provided remarkable stones recognisable to the naked eye for their pluri-centimetric white and bluish crystals. Even if small volumes of a similar marble were identified for the first time in quarries C24 and C32, the marble extracted from C25 remains distinguishable due to its unique carbon and oxygen isotopic signature. The other easily recognisable Delian marble, an orange colour dolomitic marble, appeared to be present in much larger volume than expected in quarries C23 and C24.

Concerning the other marbles, their MGS coupled with their oxygen and carbon isotopic ratio show a great potential to distinguish Delian marble from the main Mediterranean marbles. However, further analyses like REE estimation are required to discriminate unambiguously Delian marbles from other Aegean marbles such as the Parian Marathi marble or the Naxian Melanes marble.

Acknowledgment. The authors would like to thank the four-year ANR program Geology and Architecture at Delos (GAD) for granting this work. We also thank the Cyclades Ephorate for giving us the authorization to sample and analyse marbles in Delos Island. Finally, we want to thank our hosts on Delos Island for their warm hospitality during field missions.
We are grateful to the two reviewers who contributed to the improvement of this paper.

References

Altherr R, Siebel W. 2002. I-type plutonism in a continental back-arc setting: Miocene granitoids and monzonites from the central Aegean Sea, Greece. *Contrib. Miner. Petrol* 143: 397–415.

Altherr R, Schliestedt M, Okrusch M, Seidel E, Kreuzer H, Harre W, *et al.* 1979. Geochronology of high-pressure rocks on Sifnos (Cyclades, Greece). *Contrib. Miner. Petrol.* 70: 245–255. https://doi.org/10.1007/BF00375354.

Antonelli F, Lazzarini L. 2015. An updated petrographic and isotopic reference database for white marbles used in antiquity. *Rend. Fis. Acc. Lincei* 26: 399–413.

Attanasio D, Brilli M, Ogle N. 2006. The isotopic signature of classical marbles. L'Erma di Bretschneider.

Attanasio D, Bruno M, Prochaska W, Yavuz AB. 2015. A multi-method database of the black and white marbles of Göktepe (Aphrodisias), including isotopic, EPR, trace and petrographic data. *Archaeometry* 57: 217–245. https://doi.org/10.1111/arcm.12076.

Berger A, Ebert A, Ramseyer K, Gnos E, Decrouez D. 2016. Dolomite microstructures between 390 °C and 700 °C: indications for deformation mechanisms and grain size evolution. *Journal of Structural Geology* 89: 144–152. https://doi.org/10.1016/j.jsg.2016.06.001.

Bonneau M. 1982. Évolution geodynamique de l'arc egeen depuis le Jurassique superieur jusqu'au Miocene. *Bulletin de la Société Géologique de France* S7-XXIV: 229–242. https://doi.org/10.2113/gssgfbull.S7-XXIV.2.229.

Bröcker M, Franz L. 1994. The contact aureole on Tinos (Cyclades, Greece). Part I: field relationships, petrography and P-T conditions. *Mineralogy and Petrology* 54: 262–280.

Bruneau P, Ducat J. 2005. Guide de Délos, 4th ed. Sites et monuments. École française d'Athènes EFA.

Capedri S, Venturelli G. 2004. Accessory minerals as tracers in the provenancing of archaeological marbles, used in combination with isotopic and petrographic data*. *Archaeometry* 46: 517–536. https://doi.org/10.1111/j.1475-4754.2004.00171.x.

Capedri S, Venturelli G, Photiades A. 2004. Accessory minerals and $\delta^{18}O$ and $\delta^{13}C$ of marbles from the Mediterranean area. *Journal of Cultural Heritage* 5: 27–47. https://doi.org/10.1016/j.culher.2003.03.003.

Cayeux L. 1911. Description physique de l'Île de Délos. Exploration archéologique de Délos IV. Paris : Fontemoing et Cie éditeurs.

Chatzidakis P, Katzsikis G, Matarangas M. 1997. Delos sacred Greece: Characterization of the building stones, their origin an decay factor. In: *Engineering Geology and the Environment*. Leiden: CRC Press/Balkema, pp. 3089–3094.

Denèle Y, Lecomte E, Jolivet L, Lacombe O, Labrousse L, Huet B, *et al.* 2011. Granite intrusion in a metamorphic core complex: The example of the Mykonos laccolith (Cyclades, Greece). *Tectonophysics* 501: 52–70.

Fraisse P, Kozelj T. 1991. Une carrière de marbre au Sud-Est du Cynthe. *Bulletin de Correspondance Hellénique* 115: 283–296. https://doi.org/10.3406/bch.1991.4684.

Gärtner C, Bröcker M, Strauss H, Farber K. 2011. Strontium-, carbon- and oxygen-isotope compositions of marbles from the Cycladic blueschist belt, Greece. *Geological Magazine* 148: 511–528. https://doi.org/10.1017/S001675681100001X.

Gautier P, Brun J-P. 1994. Ductile crust exhumation and extensional detachments in the central Aegean (Cyclades and Evvia Islands). *Geodinamica Acta* 7: 57–85. https://doi.org/10.1080/09853111.1994.11105259.

Green WA, Young SMM, Van der Merwe NJ, Hermann JJ Jr. 2002. Source tracing marble: trace element analysis with inductively coupled plasma-mass spectrometry. Asmosia 5: Interdisciplinary Studies on Ancient Stone.

Hadjidakis P, Matarangas D, Varti-Matarangas M. 2003. Ancient quarries in Delos, Greece. ASMOSIA VII.

Herz N. 1988. The oxygen and carbon isotopic database for classical marble. In: Herz N, Waelkens M, eds. *Classical Marble: Geochemistry, Technology, Trade*. NATO ASI Series. Dordrecht: Springer Netherlands, pp. 305–314. https://doi.org/10.1007/978-94-015-7795-3_33.

Jolivet L, Brun J-P. 2010. Cenozoic geodynamic evolution of the Aegean. *Int. J. Earth Sci. (Geol. Rundsch.)* 99: 109–138. https://doi.org/10.1007/s00531-008-0366-4.

Jolivet L, Famin V, Mehl C, Parra T, Aubourg C, Hébert R, *et al.* 2004a. Strain localization during crustal-scale boudinage to form extensional metamorphic domes in the Aegean Sea. In: *Gneiss Domes in Orogeny*. Geological Society of America, pp. 185–210.

Jolivet L, Rimmelé G, Oberhänsli R, Goffé B, Candan O. 2004b. Correlation of syn-orogenic tectonic and metamorphic events in the Cyclades, the Lycian nappes and the Menderes massif.

Geodynamic implications. *Bulletin de la Société Géologique de France* 175: 217–238. https://doi.org/10.2113/175.3.217.
Jolivet L, Gorini C, Smit J, Leroy S. 2015. Continental breakup and the dynamics of rifting in back-arc basins: The Gulf of Lion margin. *Tectonics* 34: 662–679. https://doi.org/10.1002/2014TC003570.
Jolivet L, Sautter V, Moretti I, Vettor T, Papadopoulou Z, Augier R, *et al.* 2021. Anatomy and evolution of a migmatite-cored extensional metamorphic dome and interaction with syn-kinematic intrusions, the Mykonos-Delos-Rheneia MCC. *Journal of Geodynamics* 144. https://doi.org/10.1016/j.jog.2021.101824.
Keay S. 1998. The geological evolution of the Cyclades, Greece: Constraints from SHRIMP U-Pb geochronology. https://doi.org/10.25911/5d66671ad2b2f.
Kokkorou-Aleura G, Poupáki E, Efstathópoulos A, Chatzikonstantínou A. 2014. Corpus archaiōn latomeiōn: latomeia tou elladikou chōrou apo tous proïstorikous eōs tus mesaiōnikous chronous. Panepistemio Athenōn, Philosophike Schole, Tomeas Archaiologias kai Istorias tes Technes, Athena.
Kushnir ARL, Kennedy LA, Misra S, Benson P, White JC. 2015. The mechanical and microstructural behaviour of calcite-dolomite composites: An experimental investigation. *Journal of Structural Geology* 70: 200–216. https://doi.org/10.1016/j.jsg.2014.12.006.
Lazzarini L. 2004. Archaeometric aspects of white and coloured marbles used in antiquity: the state of the art. *Periodico di Mineralogia* 14.
Lepsius R. 1890. Griechische Marmorstudien. Berlin, Könige: Akademie der Wissenschaften.
Lister GS, Banga G, Feenstra A. 1984. Metamorphic core complexes of Cordilleran type in the Cyclades, Aegean Sea, Greece. *Geology* 12: 221–225. https://doi.org/10.1130/0091-7613(1984)12<221:MCCOCT>2.0.CO;2.
Lucas I. 1999. Le pluton de mykonos-delos-rhenee (cyclades, grece) : un exemple de mise en place synchrone de l'extension crustale (thesis). Orléans.
Moore AC. 1970. Descriptive terminology for the textures of rocks in granulite facies terrains. *Lithos* 3: 123–127. https://doi.org/10.1016/0024-4937(70)90067-8.
Munsell AH. 1905. A color notation. G.H. Ellis Co.
Parra T, Vidal O, Jolivet L. 2002. Relation between the intensity of deformation and retrogression in blueschist metapelites of Tinos Island (Greece) evidenced by chlorite–mica local equilibria. *Lithos* 63: 41–66. https://doi.org/10.1016/S0024-4937(02)00115-9.
Passchier CW, Trouw RAJ. 2005. Microtectonics. Springer Science & Business Media.
Pe-Piper G, Piper DJW, Matarangas D. 2002. Regional implications of geochemistry and style of emplacement of Miocene I-type diorite and granite, Delos, Cyclades, Greece. *Lithos* 60: 47–66. https://doi.org/10.1016/S0024-4937(01)00068-8.
Poretti G. 2016. In situ analysis of white marble from the Mediterranean Basin by LA-ICP-MS: inferences on provenace based on trace-element profiles.
Poretti G, Brilli M, De Vito C, Conte AM, Borghi A, Günther D, *et al.* 2017. New considerations on trace elements for quarry provenance investigation of ancient white marbles. *Journal of Cultural Heritage* 28: 16–26.
Rabillard A. 2017. Interactions magmas-détachements : du terrain (Mer Egée, Grèce) à l'expérimentation [Trad.: Magmas-detachments interactions: From field (Aegean Sea, Greece) to experimental work]. Université d'Orléans.
Rabillard A, Jolivet L, Arbaret L, Bessière E, Laurent V, Menant A, *et al.* 2018. Synextensional granitoids and detachment systems within cycladic metamorphic core complexes (Aegean Sea, Greece): Toward a regional tectonomagmatic model. *Tectonics* 37: 2328–2362. https://doi.org/10.1029/2017TC004697.
Ring U, Layer PW, Reischmann T. 2001. Miocene high-pressure metamorphism in the Cyclades and Crete, Aegean Sea, Greece: Evidence for large-magnitude displacement on the Cretan detachment. *Geol*. 29: 395. https://doi.org/10.1130/0091-7613(2001)029<0395:MHPMIT>2.0.CO;2.
Shieh YN, Taylor HP. 1969. Oxygen and Carbon isotope studies of contact metamorphism of carbonate rocks. *J. Petrol.* 10: 307–331. https://doi.org/10.1093/petrology/10.2.307.
Vallois R. 1944. L'architecture hellénique et hellénistique à Délos I. Paris.
Vettor T, Sautter V, Pont S, Harivel C, Jolivet L, Moretti I, *et al.* 2021. Delos archaeological marbles: a preliminary geochemistry-based quarry provenance study. *Archaeometry*. https://doi.org/10.1111/arcm.12655.
Zoeldfoeldi J. 2011. 5000 years marble history in troia and the troad. Petroarchaeological study on the provenance of white marbles in West Anatolia.

Cite this article as: Vettor T, Sautter V, Jolivet L, Moretti J-C, Pont S. 2022. Marble quarries in Delos Island (Greece): a geological characterization, *BSGF - Earth Sciences Bulletin* 193: 16.